Dalton Transactions

PAPER

View Article Online
View Journal

Cite this: DOI: 10.1039/c7dt03752j

Copper(I) complexes based on ligand systems with two different binding sites: synthesis, structures and reaction with O_2†

S. T. Li, B. Braun-Cula, S. Hoof and C. Limberg *

The synthesis of the ligand systems $\mathbf{L^1}$ and $\mathbf{L^2}$ with two different N_3-binding sites linked through a dibenzofuran spacer and their coordination properties towards a variety of Cu^I precursors are reported. The reaction of $\mathbf{L^1}$ with copper halides leads to the formation of a bimetallic species $[(\mathbf{L^1})(Cu^ICl)_2]$ (**1**), and metallodimers $[((\mathbf{L^1})(Cu^IX)_2)_2(\mu\text{-}(Cu^I_2)(\mu\text{-}X)_2)]$ (**2**: X = Br, **3**: X = I) in which two dicopper complexes are bridged by a $(\mu\text{-}(Cu^I_2)(\mu\text{-}X)_2)$-moiety whereas $\mathbf{L^2}$ reacts with copper chloride to afford $\{[Cu^I_2(\mathbf{L^2})Cl_2]\}_n$ (**8**). Furthermore, starting from $\mathbf{L^1}$ in combination with copper(I) salts of weakly coordinating anions the dicopper complexes $[(\mathbf{L^1})(Cu^I(NCCH_3))_2](BF_4)_2$ (**4**), $[(\mathbf{L^1})(Cu^I(NCCH_3))(Cu(Y))](Y)$ (**5**: Y = OTf, **6**: Y = ClO_4) and $[(\mathbf{L^1})(Cu^I_2(dppe))](PF_6)_2$ (**7**) were isolated, and employing $\mathbf{L^2}$, the complexes $[(\mathbf{L^2})(Cu^I(NCCH_3))_2](Z)_2$ (**9**: Z = PF_6, **10**: Z = OTf) and $[(\mathbf{L^2})(Cu^I_2(dppe))](PF_6)_2$ (**11**) were obtained. Complexes **4–6** as well as **9** and **10** react rapidly with O_2 to form metastable O_2 adducts in acetone at −90 °C, where O_2 is bound between the two copper centers within one dicopper molecule, as evidenced by UV/Vis spectroscopy, kinetic investigations, Raman spectroscopy and studies with ligands containing the isolated donor sites. The reactivity of the O_2 adducts towards selected substrates was also investigated, showing their ability to act as electrophiles as well as nucleophiles.

Received 6th October 2017,
Accepted 30th November 2017

DOI: 10.1039/c7dt03752j

rsc.li/dalton

Introduction

To achieve chemical transformations nature often uses enzymes where two metal centers cooperate. These active sites can be symmetric, as is the case, for hemocyanin (Fig. 1a),[1] but often they are unsymmetric due to two different binding pockets,[2–4] which in some enzymes even bind two different metals.[5] While it is clear that for the latter purpose unsymmetric ligand spheres are needed, it is not obvious why they are found in certain homobimetallic sites like for the dicopper unit within the pMMO (Fig. 1b).[2–4a] This motivates studies on complexes featuring two metals in different coordination environments. In the literature, there is a large number of model complexes displaying a symmetrical binuclear copper site[6,7] and they are much more explored compared to the unsymmetrical dicopper model complexes.[8–10]

Their synthesis is difficult, though, starting from the corresponding mononuclear entities, as mixtures containing the corresponding symmetric complexes are typically obtained. This problem can be circumvented by employing unsymmetric dinucleating ligands. Although their development can be syn-

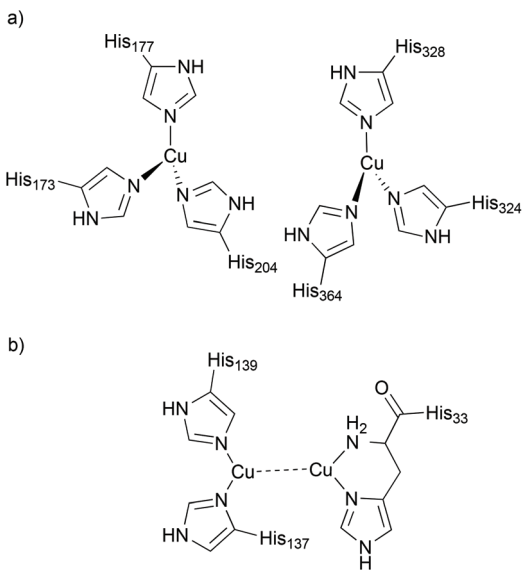

Fig. 1 Dinuclear units in the active centers of (a) hemocyanin and (b) particulate methane monooxygenase.

Department of Chemistry, Humboldt-Universität zu Berlin, Brook-Taylor-Str. 2, 12489 Berlin, Germany. E-mail: christian.limberg@chemie.hu-berlin.de; Fax: +49-30-2093-6966; Tel: +49-30-2093-7571

†Electronic supplementary information (ESI) available: ^1H NMR, ^{13}C NMR, mass, UV/Vis spectra and crystal data. CCDC 1566560–1566568. For ESI and crystallographic data in CIF or other electronic format see DOI: 10.1039/c7dt03752j

thetically rather challenging, in case of success their complexes can provide information on the cooperativity of the two different sites.[8–10] In addition, such ligands may set the basis also for the preparation of heterobimetallic units.[9–11]

Here we report synthetic routes to two novel ligands with two different binding pockets that are connected by linker units differing in one methylene group. We have chosen the biometal copper for first complexation studies and the potential of the two metals to act concertedly was tested in O_2 activation studies.

Previously, studies on bioinorganic model compounds have shown that dioxygen activation at two copper(I) centers typically leads to either a (μ-1,2)peroxodicopper(II) adduct ^{T}**P** or ^{C}**P**, a (μ–η^2:η^2)peroxo complex **P**, or a bis(μ-oxo)dicopper(III) unit **O** with a fully cleaved O–O bond (Chart 1).[12–25] Occasionally two dicopper(I) entities cooperate to form a Cu^{II}–O–Cu^{II} core.[26]

The type of Cu/O_2 species formed can be influenced by the denticity of the binding pockets.[6c] Given the tendency of Cu^{II} to five-coordination, O_2-reactive Cu^{I} complexes containing tetradentate ligands limit the binding of dioxygen to the end-on mode. In contrast, Cu^{I} complexes with bi- and tridentate ligands have more coordination flexibility and therefore enable the binding of dioxygen to the side-on mode. The formation of an **O** species is predominantly found in Cu(I) complexes with bidentate ligands as Cu^{III} ions prefer a square-planar coordination geometry. Nevertheless, Cu^{I} complexes with tridentate ligands that form **O** species are also known.[6c,21a,27] Finally the distance plays an important role. The cleavage of the O–O bond to yield in **O** requires significant impact of electron density and thus close contact of dioxygen to two Cu centres. Hence, dinucleating ligands which do not allow such a close approach will favour the formation of ^{T}**P**. Complexes of the types **P** and **O** can be a part of an equilibrium, and it has been shown that factors such as electronic and steric properties of the ligand environment,[15–18] temperature,[19,20] solvent,[16,21] concentration,[19,20] and the nature of the counterion[18a,21a,22] strongly influence the equilibrium position between **P** and **O**.[12,23–25a] Equilibria between ^{T}**P** and **O** cores have been reported, too.[25b]

We have recently reported the synthesis of two unsymmetric ligand systems containing different binding pockets and explored the O_2 chemistry of their respective dicopper complexes (Fig. 2). While for $[Cu_2(L^A)(CH_3CN)_3]^{2+}$ no O_2 adduct was detected, for $[Cu_2(L^B)(CH_3CN)_2]^{2+}$ a distinct UV/Vis band could be observed after O_2 treatment at −90 °C but the nucleo-

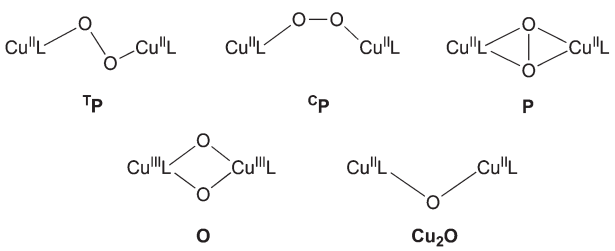

Chart 1 Possible intermediates after dioxygen activation at two copper(I) centers; L = ligand.

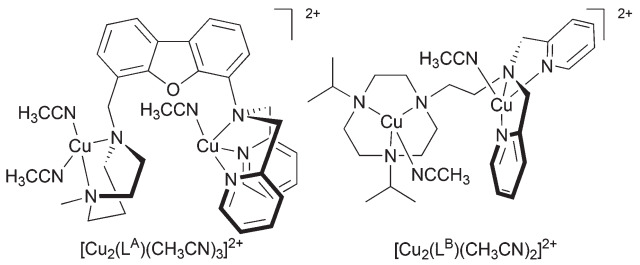

Fig. 2 Recently synthesized dicopper(I) complexes with unsymmetric dinucleating ligand systems.

arity of the formed primary O_2 adduct could not be clarified due to its short lifetime.[28]

We now describe the results obtained investigating whether the exchange of the ethylene spacer in L^B can lead to the formation of a more stable O_2 adduct in which the oxygen molecule is bound between the two copper centers within one dicopper complex. Therefore, we synthesized a ligand precursor analogous to L^B in which the ethylene spacer is replaced by a dibenzofuran backbone. Since small changes in the ligand precursor can have a crucial influence on the formed O_2 adducts,[29,30] we have also targeted the synthesis of a second ligand precursor that possesses an additional CH_2-unit between the triazacyclononane binding pocket and the dibenzofuran backbone.

Results and discussion

Ligand synthesis

The ligand synthesis relies on our recently published access to the 6-bromo-*N*,*N*-bis[(2-pyridinyl)methyl]-4-dibenzofuranamine (DBF-BrNPy_2) building block.[28,31] The potentially dinucleating ligand $\mathbf{L^1}$ was obtained *via* the Buchwald–Hartwig cross coupling of DBF-BrNPy_2 with 1,4-diisopropyl-1,4,7-triazacyclononane (iPr_2Tacn) yielding 21% of the desired product (Scheme 1). The second ligand precursor, $\mathbf{L^2}$, was synthesized *via* the Suzuki–Miyaura cross coupling of DBF-BrNPy_2 with 1,4-diisopropyl-1,4,7-triazacyclononane-7-methyltrifluoro-borate (iPr_2TacnHCH_2BF_3) in 62% yield. The identities of $\mathbf{L^1}$ and $\mathbf{L^2}$ were proved with the aid of mass spectrometry as well as NMR and IR spectroscopy; $\mathbf{L^1}$ was further characterized by elemental analysis and single crystal X-ray diffraction analysis (see ESI Fig. S1†).

Copper(I) halide complexes and their solid-state structures

In the next step, the reactivity of the ligands $\mathbf{L^1}$ and $\mathbf{L^2}$ with various Cu^{I} precursors was investigated (Scheme 2). The outcome of the reactions of $\mathbf{L^1}$ with different copper(I) halides was found to strongly depend on the metal precursor. The treatment of 2 equivalents of CuCl with one equivalent of $\mathbf{L^1}$ in acetonitrile led to the formation of yellow $[(\mathbf{L^1})(CuCl)_2]$ (**1**). Upon diffusion of diethyl ether into a concentrated acetone solution of **1** at room temperature single crystals suitable for

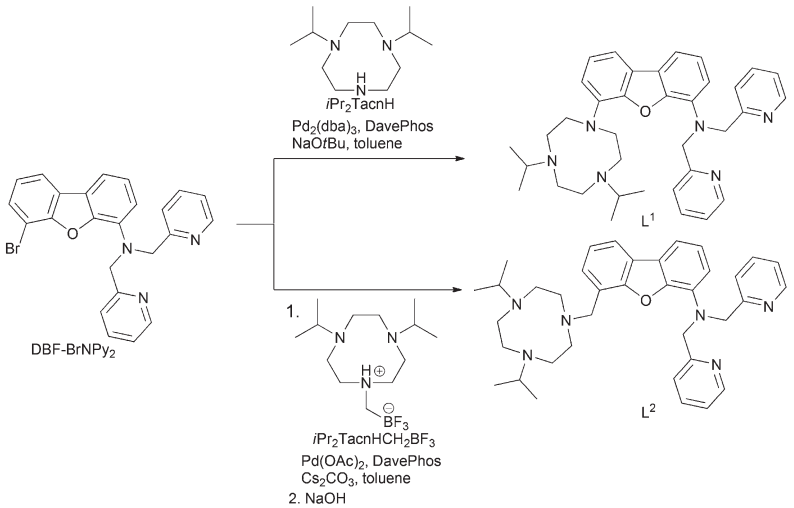

Scheme 1 Synthesis of the ligand systems L^1 and L^2.

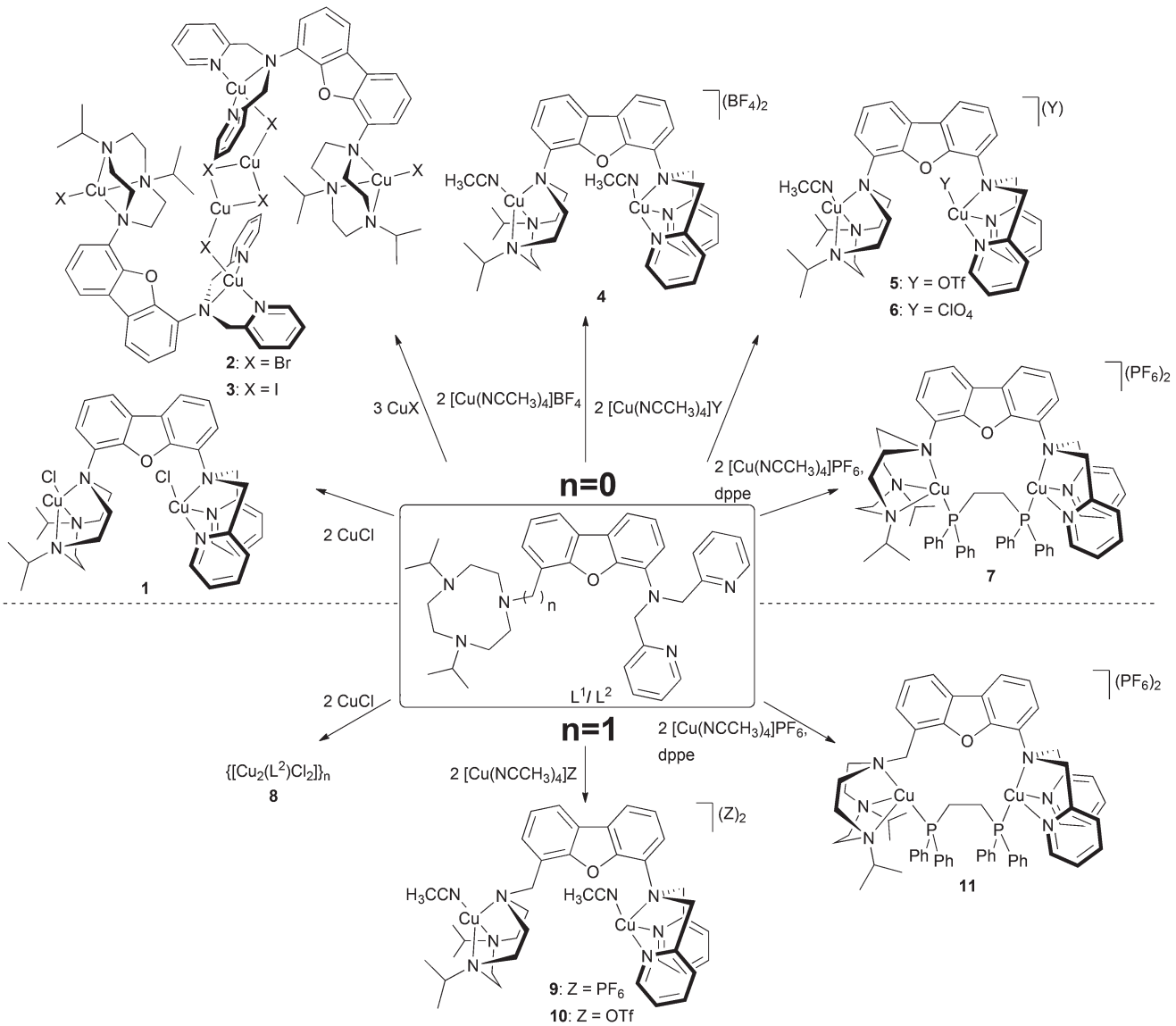

Scheme 2 Formation of Cu^I complexes of L^1 and L^2. $[Cu(NCCH_3)_4](PF_6)_2$ (2 equiv.), dppe.

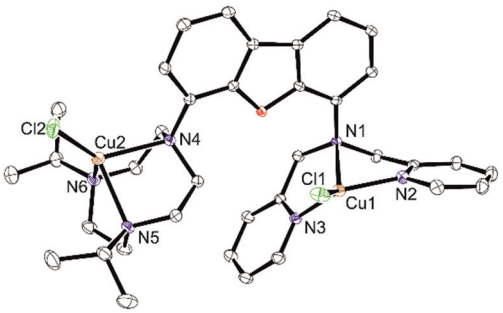

Fig. 3 Molecular structure of **1**·0.5(CH_3CN). Hydrogen atoms and the co-crystallized solvent molecules are omitted for clarity. Selected bond lengths [Å] and angles [°]: Cu1···Cu2 7.2025(6), Cu1–N1 2.5337(13), Cu1–N2 1.9882(12), Cu1–N3 1.9942(12), Cu1–Cl1 2.2327(4), Cu2–N4 2.2496(12), Cu2–N5 2.2016(12), Cu2–N6 2.1495(13), Cu2–Cl2 2.1936(4), N1–Cu1–N2 75.31(5), N1–Cu1–N3 75.09(5), N1–Cu1–Cl1 143.57(3), N2–Cu1–N3 126.56(5), N2–Cu1–Cl1 116.05(4), N3–Cu1–Cl1 114.28(4), N4–Cu2–N5 83.55(4), N4–Cu2–N6 84.24(5), N4–Cu2–Cl2 128.59(3), N5–Cu2–N6 83.72(5), N5–Cu2–Cl2 119.27(4), N6–Cu2–Cl2 139.11(4).

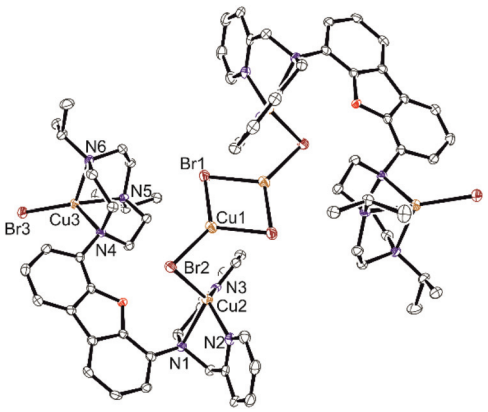

Fig. 4 Molecular structure of **2**. Hydrogen atoms are omitted for clarity. Selected bond lengths [Å] and angles [°]: Cu2···Cu3 7.3271(6), Cu2–N1 2.353(2), Cu2–N2 2.027(2), Cu2–N3 1.980(2), Cu2–Br2 2.4086(5), Cu3–N4 2.209(2), Cu3–N5 2.174(2), Cu3–N6 2.201(2), Cu3–Br3 2.3143(5), N1–Cu2–N2 79.63(9), N1–Cu2–N3 80.06(8), N1–Cu2–Br2 115.99(6), N2–Cu2–N3 125.31(10), N2–Cu2–Br2 109.28(7), N3–Cu2–Br2 125.28(7), N4–Cu3–N5 84.38(9), N4–Cu3–N6 83.27(8), N4–Cu3–Br3 127.41(6), N5–Cu3–N6 83.89(8), N5–Cu3–Br3 136.58(6), N6–Cu3–Br3 123.83(6).

crystal X-ray diffraction analysis were obtained (Fig. 3). As expected, in the molecular structure of **1** the two N_3-binding sites of $\mathbf{L^1}$ coordinate one copper(I) ion each. The copper ion of the bis(2-pyridylmethyl)amino binding site forms short bonds to the N atoms of the pyridyl donors, whereas the Cu–N_{amino} distance [Cu1–N1 2.5337(13) Å] is long in comparison to the corresponding distances found in other copper(I) chloride complexes containing the same tridentate binding pocket.[32] The Cu–N_{Tacn} bond lengths are similar to those found in other copper halide complexes featuring the triazacyclononane entity.[33] Compound **1** was further characterized by ^{1}H NMR and IR spectroscopy as well as mass spectrometry. The treatment of 2 equivalents of CuBr or CuI with one equivalent of $\mathbf{L^1}$ and appropriate work-up led to yellow products which after crystallization could be investigated by single crystal X-ray diffraction analysis. This revealed the formation of $[((\mathbf{L^1})(CuX)_2)_2(\mu\text{-}(Cu_2)(\mu\text{-}X)_2)]$ (**2**: X = Br, **3**: X = I), in which a $\mathbf{L^1}$/CuX ratio of 1 : 3 is found. Exemplarily the molecular structure of **2** is shown in Fig. 4 (for **3** see ESI Fig. S2†). In contrast to compound **1** the molecular structures of **2** and **3** contain two $\mathbf{L^1}$ ligands that bind four Cu^I centers, and the respective Cu^I centers of the bis(2-pyridylmethyl)amino binding sites are bridged by a $(\mu\text{-}(Cu_2)(\mu\text{-}X)_2)$-moiety. The formation of $(\mu\text{-}(Cu_2)(\mu\text{-}X)_2)$-moieties is often found in solid state structures of complexes formed by the reaction of copper(I) halides with neutral ligand systems.[34] The copper ions in the N_3-binding sites show distorted tetrahedral coordination geometries with Cu–N bond lengths similar to those in compound **1**. Consequently, for an efficient synthesis of **2** and **3** equivalents of CuX (X = Br, I) were employed. Both complexes were characterized by ^{1}H NMR and IR spectroscopy, as well as mass spectrometry and elemental analysis. The treatment of one equivalent of $\mathbf{L^2}$ with two equivalents of CuCl and subsequent work-up also yielded a yellow solid which was analyzed by NMR and IR spectroscopy as well as mass spectrometry. Since no crystals suitable for X-ray diffraction analysis could be obtained, a monomeric, dimeric, or polymeric structure is conceivable as found for **1–3** and other copper(I) complexes with copper halide units.[34]

Dicopper(I) complexes with weakly coordinating anions and their solid-state structures

The presence of halide anions can prevent the potential binding/activation of molecules by metal complexes. They can be bound to the metal centers very tightly and thus block the access of substrates due to the lack of free coordination sites. Consequently, for activation studies, we pursued the synthesis of copper(I) complexes of $\mathbf{L^1}$/$\mathbf{L^2}$ containing weakly coordinating anions. The reaction of the ligands $\mathbf{L^1}$ and $\mathbf{L^2}$ with various copper precursors containing weakly coordinating anions in acetonitrile led to the formation of five air-sensitive dicopper complexes (*i.e.* **4–6**, **9**, **10**; Scheme 2). The use of different copper salts was of interest since the counteranions can play a perceptible role in the reactivity towards dioxygen.[18a,22] Using $\mathbf{L^1}$ the complexes $[(\mathbf{L^1})(Cu(NCCH_3))_2](BF_4)$ (**4**), $[(\mathbf{L^1})(Cu(NCCH_3))(Cu(OTf))](OTf)$ (**5**) and $[(\mathbf{L^1})(Cu(NCCH_3))(Cu(ClO_4))](ClO_4)$ (**6**) were synthesized. With the ligand $\mathbf{L^2}$, the complexes $[(\mathbf{L^2})(Cu(NCCH_3))_2](PF_6)_2$ (**9**) as well as $[(\mathbf{L^2})(Cu(NCCH_3))_2](OTf)_2$ (**10**) were isolated. All complexes were characterized by NMR and IR spectroscopy as well as by mass spectrometry, and in the cases of **4–6** and **9** also by elemental analysis. Complexes **4**, **6** and **9** were furthermore characterized by single crystal X-ray diffraction analysis. Suitable crystals of **4** were obtained by the diffusion of diethyl ether into a concentrated acetonitrile solution of **4** at room temperature (Fig. 5). Complex **4** crystallizes in the centrosymmetric space group $P2_1/c$. Each copper(I) ion is coordinated by the respective N_3-binding site and one additional exogenous acetonitrile molecule. Both copper ions show distorted tetrahedral coordination

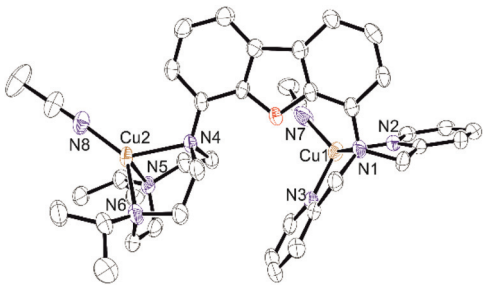

Fig. 5 Molecular structure of **4**. Hydrogen atoms and $[BF_4]^-$ anions are omitted for clarity. Selected bond lengths [Å] and angles [°]: Cu1···Cu2 7.1642(9), Cu1–N1 2.349(4), Cu1–N2 2.015(4), Cu1–N3 1.996(4), Cu1–N7 1.903(4), Cu2–N4 2.164(3), Cu2–N5 2.151(4), Cu2–N6 2.107(4), Cu2–N8 1.866(4), N1–Cu1–N2 80.00(14), N1–Cu1–N3 78.87(14), N1–Cu1–N7 129.1(2), N2–Cu1–N3 125.83(15), N2–Cu1–N7 113.62(19), N3–Cu1–N7 118.45(17), N4–Cu2–N5 86.01(13), N4–Cu2–N6 86.37(14), N4–Cu2–N8 131.38(17), N5–Cu2–N6 86.31(17), N5–Cu2–N8 117.08(16), N6–Cu2–N8 133.82(18).

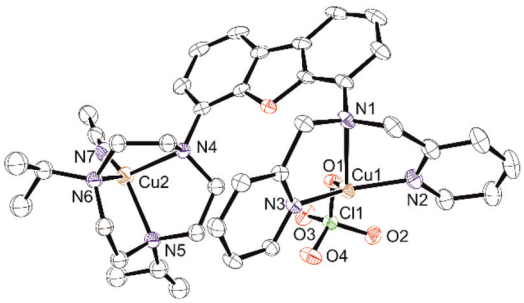

Fig. 6 Molecular structure of **6**·$C_4H_{10}O$. Hydrogen atoms, the co-crystallized solvent molecule and the non-coordinating $[ClO_4]^-$ anion are omitted for clarity. Selected bond lengths [Å] and angles [°]: Cu1···Cu2 7.1077(10), Cu1–N1 2.312(3), Cu1–N2 1.956(3), Cu1–N3 1.937(2), Cu1–O1 211(2), Cu2–N4 2.193(18), Cu2–N5 2.169(6), Cu2–N6 2.055(11), Cu2–N7 1.874(3), N1–Cu1–N2 82.11(10), N1–Cu1–N3 82.83(10), N1–Cu1–O1 115.50(8), N2–Cu1–N3 141.00(11), N2–Cu1–O1 100.55(10), N3–Cu1–O1 118.41(9), N4–Cu2–N5 85.1(3), N4–Cu2–N6 86.3(5), N4–Cu2–N7 123.3(3), N5–Cu2–N6 87.4(2), N5–Cu2–N7 131.37(19), N6–Cu2–N7 128.5(2).

geometries. The copper center of the bis(2-pyridylmethyl)amino binding site forms short bonds to the N atoms of the acetonitrile and pyridyl donors, and as in **1** the $Cu–N_{amino}$ distance [Cu1–N1 2.349(4) Å] is comparatively long.[8a,35] The $Cu–N_{Tacn}$ bonds [2.107(4)–2.164(3) Å] fall into the expected range.[20,36]

The ^1H NMR spectrum of **4** in acetonitrile-d_3 shows the complete set of signals expected for $\mathbf{L^1}$. Moreover, a singlet at 1.96 ppm is observed, that is, at a shift identical to the one found for free acetonitrile. This indicates a dynamic exchange of the coordinated CH_3CN ligands with the corresponding trideuterated CD_3CN solvent molecule and, thus, the desired lability of these co-ligands. For complexes **5** and **6** similar ^1H NMR spectra were obtained, but from the integral it can be inferred that in contrast to **4** in **5** and **6** only one of the copper centers coordinates a labile acetonitrile molecule. This could be further confirmed by the analysis of suitable crystals of **6**·$C_4H_{10}O$, which were obtained by the diffusion of diethyl ether into a concentrated acetone solution of **6** at room temperature (Fig. 6). Complex **6**·$C_4H_{10}O$ crystallizes in the centrosymmetric space group *Pbca* with each copper ion coordinated by the respective N_3-binding site. Whereas in **4** the coordination spheres of both copper ions are completed by one acetonitrile molecule each, in the case of **6**·$C_4H_{10}O$ the copper ion of the bis(2-pyridylmethyl)amino binding site is coordinated by a perchlorate anion. The coordination geometries of the copper centers as well as the Cu–N bond lengths are similar to those in compound **4**. The structure of **5** will also be similar, with triflate coordinating instead of perchlorate. The coordination of the triflate and perchlorate anions to the copper centers is not unusual: due to their oxygen atoms, both the perchlorate and the triflate anions show a stronger tendency to come into contact with metal centers compared to anions with fluorine atoms such as tetrafluoroborate or hexafluorophosphate anions.[37] The latter possess lower basicities and therefore in complex **4** instead of the tetrafluoroborate anions two acetonitrile molecules are coordinated to the copper centers. Complexes **4–6** are soluble in acetonitrile and acetone and show distinct sensitivity against dioxygen.

Suitable crystals of **9** were obtained by the diffusion of diethyl ether into a concentrated solution of **9** in acetonitrile at room temperature (Fig. 7). Complex **9** crystallizes in the centrosymmetric space group *P*2/*n* with coordination geometries of the copper centers and Cu–N bond lengths similar to those found in compounds **4** and **6**. Complex **9** is soluble in acetonitrile as well as acetone and shows distinct sensitivity against oxygen similar to complexes **4–6**. The ^1H NMR spectrum of **9** in acetonitrile-d_3 shows the complete set of signals expected for $\mathbf{L^2}$. As observed upon the dissolution of **4–6**, a singlet at 1.96 ppm is also detected in the case of **9**, which can be assigned to two uncoordinated acetonitrile molecules.

For complex **10**, a similar ^1H NMR spectrum was observed. However, in contrast to the one recorded for the $\mathbf{L^1}$-based

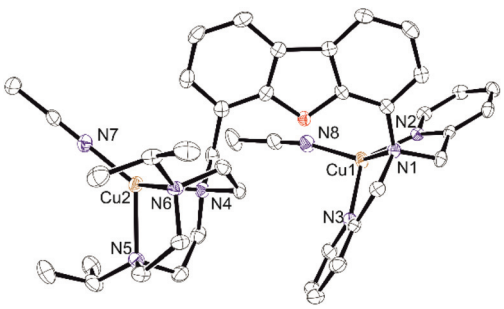

Fig. 7 Molecular structure of **9**. Hydrogen atoms and the $[PF_6]^-$ anions are omitted for clarity. Selected bond lengths [Å] and angles [°]: Cu1···Cu2 7.9571(8), Cu1–N1 2.3459(19), Cu1–N2 1.989(2), Cu1–N3 2.045(2), Cu1–N8 1.933(2), Cu2–N4 2.130(2), Cu2–N5 2.131(2), Cu2–N6 2.1332(19), Cu2–N7 1.857(2), N1–Cu1–N2 80.33(7), N1–Cu1–N3 78.83(7), N1–Cu1–N8 131.44(8), N2–Cu1–N3 129.01(8), N2–Cu1–N8 125.29(8), N3–Cu1–N8 103.08(9), N4–Cu2–N5 85.67(8), N4–Cu2–N6 86.33(7), N4–Cu2–N7 132.48(9), N5–Cu2–N6 86.03(8), N5–Cu2–N7 129.13(8), N6–Cu2–N7 122.15(8).

copper triflate complex **5** the integral of the signal belonging to the free acetonitrile indicates the presence of two acetonitrile molecules in **10**, which in this case are apparently favoured by both Cu centers in **10** over the triflate ion.

Dicopper(I) complexes with 1,2-bis(diphenylphosphino)-ethane as a bridging ligand

In the molecular structures of **1–4**, **6** and **9** the two copper centers within one dicopper molecule are not oriented towards each other. However, for the activation of small molecules it is crucial that they can cooperate. To check whether complexes of $\mathbf{L^1}$ and $\mathbf{L^2}$, with respect to geometric arguments, allow for an activation of small substrates between the metal ions within one complex molecule, the syntheses of dicopper(I) complexes where the copper centers are connected by a bridging ligand were pursued. Using two equivalents of $[Cu(NCCH_3)_4]PF_6$, one equivalent of 1,2-bis(diphenylphosphino)ethane (dppe) as well as one equivalent of $\mathbf{L^1}$, the dicopper complex $[(\mathbf{L^1})(Cu_2(dppe))](PF_6)_2$ (**7**) was synthesized. The treatment of compound **9** with one equivalent of dppe after work-up led to the formation of $[(\mathbf{L^2})(Cu_2(dppe))](PF_6)_2$ (**11**). Both complexes were characterized by IR spectroscopy and mass spectrometry, and in the case of **11** also by elemental analysis. Crystals, suitable for X-ray diffraction analysis could be obtained by the diffusion of diethyl ether into a concentrated solution of the respective complex in acetonitrile (Fig. 8). Complex $\mathbf{7}\cdot(C_4H_{10}O)\cdot(C_3H_6O)$ crystallizes in the centrosymmetric space group $P\bar{1}$. Each copper ion is coordinated by the respective N_3-binding site and one phosphorus atom of the dppe-bridging ligand. The copper ions show distorted tetrahedral coordination geometries and possess Cu–N-bond lengths similar to those obtained for **4**, **6** and **9**. Due to the dppe ligand the two copper ions are bridged, resulting in a copper–copper distance of 6.176(3) Å *i.e.* significantly shorter as compared to the copper–copper distances in **4** and **6**. Complex **11** crystallizes in the same centrosymmetric space group as $\mathbf{7}\cdot(C_4H_{10}O)\cdot(C_3H_6O)$ and shows analogous binding parameters.

It becomes obvious that a shorter bridging ligand can bring together the two copper-units within one molecule even closer and that, thus, concerning geometric arguments, the $\mathbf{L^1}$ and $\mathbf{L^2}$ systems allow for the activation of small substrates between the coordinated metal ions within a dicopper complex.

Reactivity towards dioxygen

Considering that dinuclear copper proteins in nature are mostly utilized for the activation of O_2, the O_2 reactivity of complexes **4–6**, **9** and **10** was investigated. First **4**, **5** or **6** were dissolved in acetone and injected into an oxygen-saturated dry acetone solution at −90 °C. The changes in the UV/Vis spectra of the resulting solutions were monitored, which revealed the development of one intensive absorption band at 396 nm (ε = 5600 M^{-1} cm^{-1} for **4**, 9400 M^{-1} cm^{-1} for **5** and 5800 M^{-1} cm^{-1} for **6**) for all three complexes. The identical position of the absorption band indicates the formation of the same Cu_2/O_2 species for **4–6**. Representatively, the UV/Vis spectra recorded during the reaction of **5** with O_2 are shown in Fig. 9a.

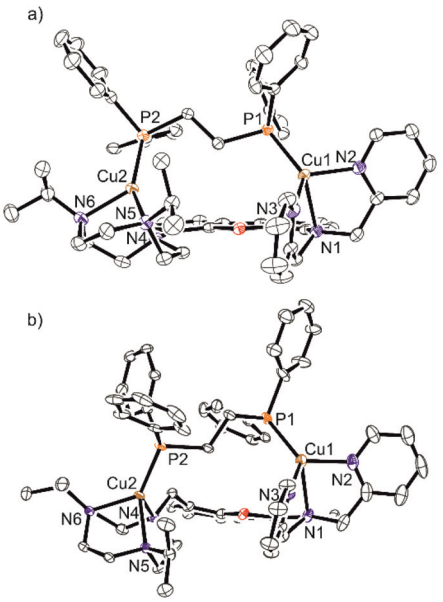

Fig. 8 Molecular structure of (a) $\mathbf{7}\cdot(C_4H_{10}O)\cdot(C_3H_6O)$. Hydrogen atoms, the co-crystallized solvent molecules and the $[PF_6]^-$ anions are omitted for clarity. Selected bond lengths [Å] and angles [°]: Cu1···Cu2 6.176(3), Cu1–N1 2.280(3), Cu1–N2 2.035(3), Cu1–N3 2.035(3), Cu1–P1 2.1765 (19), Cu2–N4 2.298(3), Cu2–N5 2.151(3), Cu2–N6 2.117(3), Cu2–P2 2.1714(16), N1–Cu1–N2 80.77(12), N1–Cu1–N3 78.54(12), N1–Cu1–P1 133.61(9), N2–Cu1–N3 115.70(13), N2–Cu1–P1 115.79(10), N3–Cu1–P1 122.43(10), N4–Cu2–N5 83.67(12), N4–Cu2–N6 86.23(12), N4–Cu2–P2 115.22(9), N5–Cu2–N6 84.55(13), N5–Cu2–P2 140.98(9), N6–Cu2–P2 128.16(10); (b) molecular structure of **11**. Hydrogen atoms and the $[PF_6]^-$ anions are omitted for clarity. Selected bond lengths [Å] and angles [°]: Cu1···Cu2 6.4451(7), Cu1–N1 2.411(2), Cu1–N2 2.024(3), Cu1–N3 2.043(2), Cu1–P1 2.1798(8), Cu2–N4 2.170(2), Cu2–N5 2.164(2), Cu2–N6 2.113(2), Cu2–P2 2.1679(7), N1–Cu1–N2 79.24(10), N1–Cu1–N3 76.26(9), N1–Cu1–P1 132.88(6), N2–Cu1–N3 108.28(10), N2–Cu1–P1 127.68(8), N3–Cu1–P1 118.05(7), N4–Cu2–N5 84.44(8), N4–Cu2–N6 84.40(9), N4––Cu2–P2 119.57(6), N5–Cu2–N6 85.56(9), N5–Cu2–P2 133.47(6), N6–Cu2–P2 132.33(6).

Under the same conditions the reactions of **9** and **10** with dioxygen were investigated by UV/Vis spectroscopy revealing an absorption band at 393 nm (ε = 9400 M^{-1} cm^{-1} for **9**, 9200 M^{-1} cm^{-1} for **10**). Representatively the UV/Vis spectra recorded during the reaction of **9** with O_2 are shown in Fig. 9b. The position of the absorption band is similar to the one observed after the oxygenation of **4–6** and thus indicates the formation of the same Cu_2/O_2 adduct, independent of the ligand system $\mathbf{L^1}$ or $\mathbf{L^2}$. In all cases after the absorption band has reached its highest intensity, the intensity decreases again, indicating that the formed Cu_2/O_2 adduct is a metastable species ($t_{1/2}$ = 3780 s for **4**, 2565 s for **5**, 4100 s for **6**, 3985 s for **9** and 4955 s for **10**). When propionitrile or other solvent mixtures such as acetone with propionitrile, CH_2Cl_2, THF or toluene were used no reaction could be observed.

The UV/Vis spectroscopic features of the Cu_2/O_2 adducts of **4–6** as well as **9** and **10** strongly indicate the formation of a bis

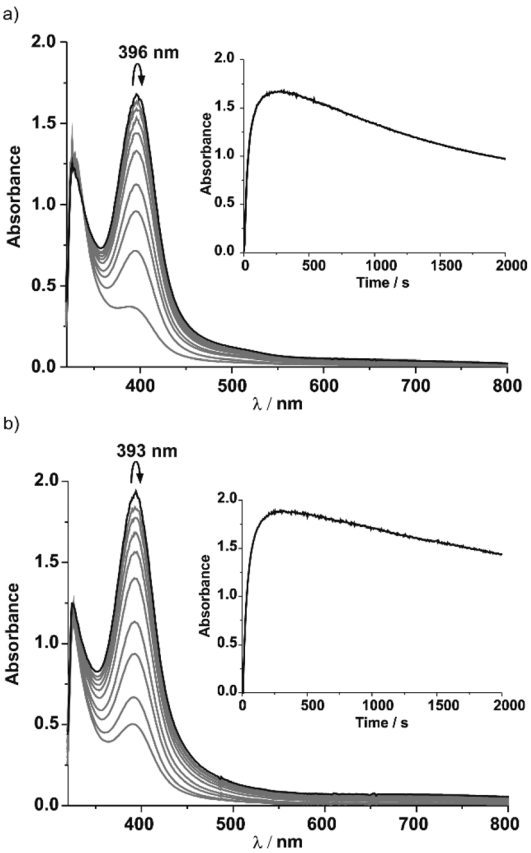

Fig. 9 UV/Vis absorption spectra for the reaction of (a) **5** (0.18 mM) with O_2 in acetone at −90 °C. The different graphs represent the spectra recorded at 5, 15, 25, 35, 55, 75, 95, 125, 155 and 200 s after addition of **5** (dissolved in 0.2 mL acetone) into an oxygen-saturated dry acetone solution (2.8 mL) (inset). The inserted plot shows the time trace at 396 nm; (b) **9** (0.2 mM) with O_2 in acetone at −90 °C. The different graphs represent the spectra recorded at 10, 15, 25, 35, 55, 75, 95, 125, 155 and 255 s after addition of **9** (dissolved in 0.2 mL acetone) into an oxygen-saturated dry acetone solution (2.8 mL). The inserted plot shows the time-trace at 393 nm.

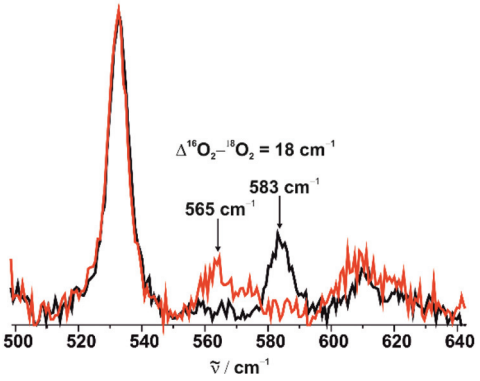

Fig. 10 Resonance Raman spectra of a 5 mM solution of **10** in acetone after oxygenation with $^{16}O_2$ (black line) and $^{18}O_2$ (red line).

(μ-oxo)dicopper(III) core (**O** core).[12,21b,30,38] This could also be confirmed by resonance Raman spectroscopic studies on compound **10** (Fig. 10).

Whereas resonance Raman experiments did not lead to the observation of isotope sensitive signals for the O_2 adducts of **4–6** when λ = 413 nm laser excitation was applied, a solution of **10** after treatment with dioxygen at −90 °C in acetone exhibited a weak vibrational feature at $\tilde{\nu}$ = 583 cm^{-1}. The latter experienced a [Δ $^{18}O_2$–$^{16}O_2$] ~18 cm^{-1} downshift when $^{18}O_2$ was employed in the oxygenation reaction. This isotope sensitive signal is characteristic of the symmetric breathing mode of the Cu_2O_2 core.[12,21,30,38]

Having clarified that O_2-activation leads to an **O** species, the next question concerns the origin of the activating sites. In principle a variety of structural motifs are conceivable (Scheme 3). Either O_2 is fixed between the two copper centers of one dicopper molecule (Scheme 3a), or between two copper ions belonging to two different molecules. The latter may lead to the formation of dimeric or oligomeric/polymeric species assuming that both binding sites activate O_2 (Scheme 3b, c, f and g). In case only one of the binding units can activate O_2, the two other copper(I) centers may also remain dangling (Scheme 3d and e).

To distinguish between these possibilities we first synthesized the mononuclear copper complexes [(DBF-BrNPy$_2$)Cu(NCCH$_3$)](OTf) (**12**) and [(DBF-HTacn)Cu(NCCH$_3$)](OTf) (**13**) with dibenzofuran backbones bearing only one of the two binding sites (Fig. 11) and tested their reactivities towards O_2. Upon contact of **12** in various solvents at −90 °C with O_2 no adduct formation could be detected by UV/Vis spectroscopy. In contrast, the injection of a solution of **13** in acetone into an oxygen-saturated dry acetone solution at −90 °C showed the development of one intense absorption band at 427 nm (ε = 9000 M^{-1} cm^{-1}) (Fig. 12a) whose position differs strongly from the bands at 396 nm and 393 nm which are observed after the oxygenations of **4**, **5** and **6** as well as **9** and **10**.

Under the same conditions the formation of an absorption band with a maximum at 394 nm (ε = 9700 M^{-1} cm^{-1}) could be observed when a 1 : 1 mixture of **12** and **13** was employed (Fig. 12b). These findings exclude that the O_2 treatment of **5–6**, **9** and **10** has led to the formation of a Cu_2/O_2 species in which the same Cu^I units of different molecules have activated O_2 between each other (Scheme 3b, d, e and f).

For further investigations, kinetic studies on the oxygenation rate of **5** and **9** were performed by UV/Vis spectroscopy. The oxygenation of both complexes in acetone at −90 °C proceeds with rapid accumulation of the **O** species (over *ca.* 200 s for **5** and 255 s for **9**) immediately followed by decomposition (see Fig. 9). The latter however is much slower than the formation so that reproducible kinetic parameters could be obtained.[27] The oxygenation rate of **5** and **9** was readily fitted by a single-exponential function and is invariant with a change in the initial copper concentration resulting in k_{obs} = 4.87 × 10^{-2} s^{-1} for **5** and 3.98 × 10^{-2} s^{-1} for **9**.[27]

The observed first-order process and the concentration independence suggest that the formation of the Cu_2/O_2 adduct does not require more than one equivalent of the starting com-

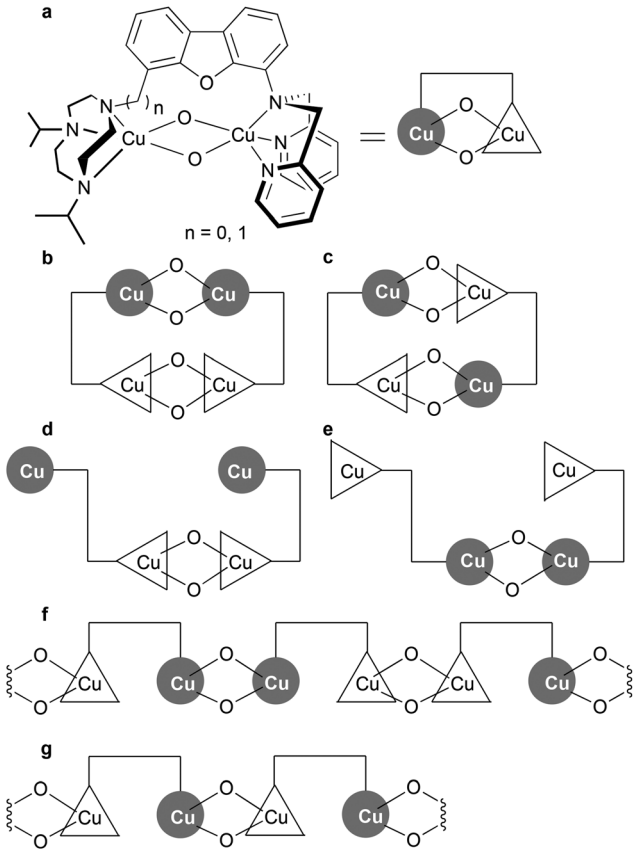

Scheme 3 Representation of conceivable structures for the Cu_2/O_2 adducts, obtained after the reaction of **4**, **5** or **6** with dioxygen. (a) Monomeric species, (b) dimeric species in which the same or (c) different Cu^I units of two different molecules have activated O_2 between each other, (d) dimeric species in which only the $[Cu(iPr_2Tacn)]^+$ unit or (e) the $[Cu(bis(2\text{-pyridylmethyl})amino)]^+$ unit has reacted, and (f) oligomeric/polymeric species in which the same or (g) different Cu^I units have reacted.

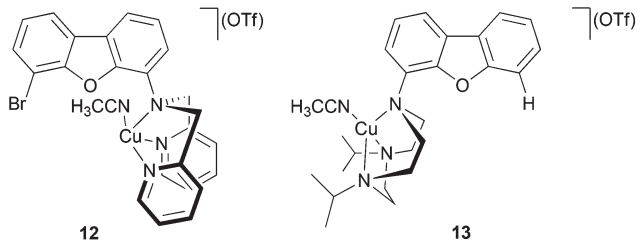

Fig. 11 Mononuclear copper(I) complexes **12** and **13** bearing the bis(2-pyridylmethyl)amino or the triazacyclononane binding site only.

plexes and therefore indicate the formation of Cu_2/O_2 adducts in the ratio 1 : 1 for **4**, **5** and **6** as well as for **9** and **10**.

The **O** species formed from **4–6** as well as **9** and **10** are unstable even at −90 °C. All attempts to crystallize these primary products or any of the decay products were unsuccessful. To check whether the source of instability is an oxidation of the ligand by the reactive Cu_2O_2 unit, exemplarily an oxygenated solution of **4** in acetone was treated with an ethylenediaminetetraacetic acid (EDTA) buffer (10 mM H_4EDTA, 27 mM NaAc, and 0.04 mM HAc) under aerobic conditions. Subsequently $\mathbf{L^1}$ was recovered as the main product, as confirmed by ^{1}H NMR spectroscopy and mass spectrometry.

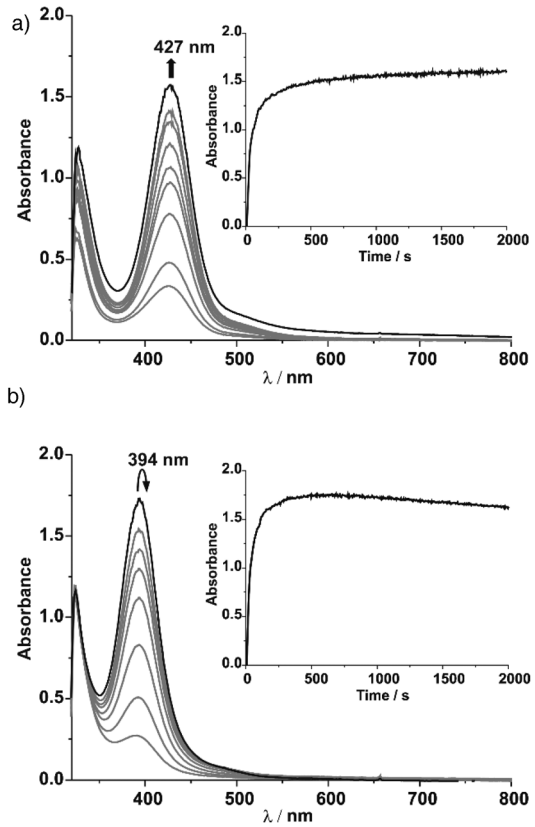

Fig. 12 UV/Vis absorption spectra for the reaction of (a) **12** (0.18 mM) with O_2 in acetone at −90 °C. The different graphs represent the spectra recorded at 5, 10, 20, 40, 60, 90, 190, 290 and 1160 s after the addition of **12** (dissolved in 0.2 mL acetone) into an oxygen-saturated dry acetone solution (2.8 mL) (inset). The inserted plot shows the time trace at 427 nm; (b) a 1 : 1 mixture of **12** and **13** (0.18 mM) with O_2 in acetone at −90 °C. The different graphs represent the spectra recorded at 5, 10, 20, 40, 60, 90, 120 and 485 s after addition of **12** and **13** (dissolved in 0.2 mL acetone) into an oxygen-saturated dry acetone solution (2.8 mL). The inserted plot shows the time-trace at 394 nm.

Reactivity with exogenous substrates

We also investigated the reactivity of the **O** adduct of complexes **5** and **9**, $[(\mathbf{L^1})Cu_2O_2]^{2+}$ and $[(\mathbf{L^2})Cu_2O_2]^{2+}$, towards selected substrates (Scheme 4).

In general, the Cu_2O_2 moieties in **O** adducts have been shown to act as electrophiles. Consistent with this observation $[(\mathbf{L^1})Cu_2O_2]^{2+}$ and $[(\mathbf{L^2})Cu_2O_2]^{2+}$ were able to perform oxygen transfer to triphenylphosphine as well as hydrogen atom abstraction from the C–H (or O–H) bond of xanthene and 2,4-di-*tert*-butylphenol, respectively, resulting in the formation of xanthone and 3,3′,5,5′-tetra-*tert*-butyl-2,2′-bis(phenol). UV/Vis monitoring and kinetic analysis revealed that the addition of triphenylphosphine to $[(\mathbf{L^1})Cu_2O_2]^{2+}$ resulted in instantaneous disappearance of the absorption band at 393 nm. For the same

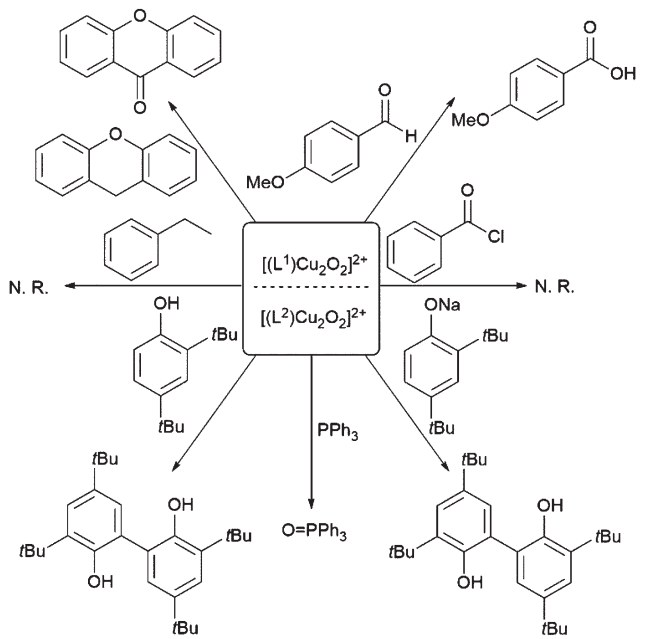

Scheme 4 Reactivity of $[(\mathbf{L^1})Cu_2O_2]^{2+}$ and $[(\mathbf{L^2})Cu_2O_2]^{2+}$ towards exogenous substrates. (N.R. = no reaction).

reaction with $[(\mathbf{L^2})Cu_2O_2]^{2+}$ a pseudo-first order decay of the absorption feature at 396 nm was observed. The rate constant increases proportionally with the substrate concentration, affording a second rate constant, k_2, of 0.2050 M^{-1} s^{-1}.

No reactivity was observed in contact with ethylbenzene probably due to its higher bond dissociation energy (BDE = 87 kcal mol^{-1}) compared to xanthene (BDE = 74 kcal mol^{-1}).[39] Furthermore, no tyrosinase-like reactivity was observed when the sodium salt of 2,4-di-*tert*-butylphenolate was reacted with $[(\mathbf{L^1})Cu_2O_2]^{2+}$ and $[(\mathbf{L^2})Cu_2O_2]^{2+}$; instead 3,3′,5,5′-tetra-*tert*-butyl-2,2′-bis(phenol) was formed. The above observations indicate the potential of $[(\mathbf{L^1})Cu_2O_2]^{2+}$ and $[(\mathbf{L^2})Cu_2O_2]^{2+}$ to act as electrophilic oxidants. However, they also react with 4-methoxybenzaldehyde to generate the corresponding benzoic acid in quantitative yield. Thus, similar to the reaction of $[(\mathbf{L^1})Cu_2O_2]^{2+}$ or $[(\mathbf{L^2})Cu_2O_2]^{2+}$ with triphenylphosphine, UV/Vis monitoring showed that $[(\mathbf{L^1})Cu_2O_2]^{2+}$ reacts much faster with 4-methoxybenzaldehyde (k_2 = 3.68079 M^{-1} s^{-1}) than $[(\mathbf{L^2})Cu_2O_2]^{2+}$ (k_2 = 0.5769 M^{-1} s^{-1}), showing that minor ligand alterations can affect the reactivity of the copper–dioxygen complexes.

When benzoylchloride was employed no reaction was observed. Such an ambivalent behavior was observed before[25b] and might be due to an equilibrium between **O** and $^{\mathbf{T}}\mathbf{P}$ species even though a $^{\mathbf{T}}\mathbf{P}$ species could not be detected when complexes **4–6** as well as **9** and **10** were treated with dioxygen.

Conclusions

We report the synthesis of two novel asymmetric dinucleating ligand systems $\mathbf{L^1}$ and $\mathbf{L^2}$ with tridentate binding sites linked through a dibenzofuran spacer. The ligand systems differ by one additional CH_2 group in $\mathbf{L^2}$ between the backbone and the cyclic N_3-binding site. $\mathbf{L^1}$ and $\mathbf{L^2}$ were successfully employed for the synthesis of copper(I) complexes. The dicopper compounds **4–6** as well as **9** and **10** with weakly coordinating anions were then investigated with respect to their behaviour towards O_2. For all complexes the formations of a metastable **O** adduct could be observed by UV/Vis spectroscopy. The **O**-type structure has been further established by resonance Raman spectroscopy performed with the O_2 adduct of **10**. The nature of the **O** species has been further studied with the aid of kinetic measurements on the oxygenation rates of **5** and **9** showing no dependency of the pseudo-first-order rate constant on the initial copper concentration. Moreover, UV/Vis measurements employing the mononuclear complexes **12** and **13**, containing only one of the two binding sites, with O_2 clearly showed that only the reaction of two different Cu^I units leads to an absorption band observed for the **O** species of **4–6** as well as **9** and **10**. Both the **O** adducts of **5** and **9**, $[(\mathbf{L^1})Cu_2O_2]^{2+}$ and $[(\mathbf{L^2})Cu_2O_2]^{2+}$, were able to perform electrophilic as well as nucleophilic reactions. The differences in the ligand systems $\mathbf{L^1}$ and $\mathbf{L^2}$ do not strongly affect the electronic structure or the principal reactivity of the formed Cu_2/O_2 adducts. Nevertheless, the rate towards the reaction with triphenylphosphine and 4-methoxybenzaldehyde is significantly different for $[(\mathbf{L^1})Cu_2O_2]^{2+}$ and $[(\mathbf{L^2})Cu_2O_2]^{2+}$ indicating that small changes in the ligand system can have a crucial influence on the reaction behavior of the copper-dioxygen complexes. Including the results of former work[28] the new insights gained here clearly show that the available binding pockets and the freedom, which the backbone provides them for cooperation, determine the Cu_2/O_2 systems. Both ligand systems reported here offer a good platform for the future synthesis of heterodinuclear complexes that may exhibit novel spectroscopic properties, electronic structures, and reactivities in comparison to their homometallic analogues.

Experimental section

General

All manipulations with air-sensitive compounds were carried out in a glove box or by means of Schlenk-type techniques involving a dry and oxygen-free argon atmosphere. The NMR spectra were recorded with Bruker DPX 300 (^{19}F 282.4 MHz) AV 400 (^{1}H 400.1 MHz, ^{13}C 100.6 MHz, ^{31}P 162.0 MHz), and AV 500 (^{1}H 500.1 MHz, ^{13}C 125.8 MHz, ^{19}F 470.6 MHz) NMR spectrometers in CD_3CN, CD_2Cl_2 or $CDCl_3$ at 25 °C. The ^{1}H NMR spectra were calibrated against the internal residual proton and natural abundance ^{13}C resonances of the deuterated solvent. The ^{19}F NMR spectra were calibrated against the external standard $CFCl_3$ or H_3PO_4 for ^{31}P NMR spectra. Chemical shifts and coupling constants (J) were reported in parts per million (δ) and hertz, respectively. The assignment of signals was done with the help of 2D experiments. Microanalyses were performed with a HEKAtech Euro EA 3000 elemental analyzer.

Only selected peaks in the mass spectra are reported below. Infrared (IR) spectra were recorded with samples prepared as KBr pellets in the region of 4000–400 cm^{-1} with a Shimadzu FTIR 8400S. ATR-FTIR spectra were recorded with a Bruker Alpha in a region of 4000–400 cm^{-1} using dissolved samples after the solvent was evaporated. ESI-MS spectra were recorded with an Agilent Technologies 6210 TOF-LC-MS. UV/Vis spectra were obtained at variable temperatures on an Agilent 8453 UV/Visible spectrophotometer equipped with a Unisoku USP-203-A cryostat. SUPRASIL® Quartz cells from Hellma Analytics with a 10 mm path length were used. Resonance Raman spectra were recorded in acetone at −90 °C (Bruker cryostat) using 413 nm excitation (Kr^+-laser) with a Horiba Jobin–Yvon LabRAM HR800 confocal Raman spectrometer. The concentration of the sample was 5 mM.

Materials

Unless otherwise stated, all starting materials were obtained from commercial sources with the highest possible grade of purity and used without further purification. 6-Bromo-*N*,*N*-bis[(2-pyridinyl)methyl]-4-dibenzofuranamine (DBF-BrNPy$_2$),[28,31] 1,4-diisopropyl-1,4,7-triazacyclononane[40] and dibromodibenzofuran[31] were prepared according to a literature procedure. $[Cu(NCCH_3)_4]PF_6$ was prepared according to a literature procedure.[41] By variation of the previous literature method, $[Cu(NCCH_3)_4]X$ (X = SO_3CF_3, BF_4, ClO_4) was synthesized from Cu_2O and trifluoromethanesulfonate acid, tetrafluoroboric acid, or perchloric acid. Purification by column chromatography was performed with aluminum oxide purchased from Sigma-Aldrich (activated, neutral, Brockmann Activity I, 0.05–0.15 mm). Solvents were dried by using an MBraun Solvent Purification System SPS.

Ligand synthesis

L^1: A Schlenk flask was charged with DBF-BrNPy$_2$ (724 mg, 1.63 mmol), TacnH (0.43 mL, 1.79 mmol, 1.1 equiv.), $Pd_2(dba)_3$ (75 mg, 0.08 mmol, 0.05 equiv.), DavePhos (64 mg, 0.16 mmol, 0.1 equiv.) and sodium *tert*-butoxide (234 mg, 2.44 mmol, 1.5 equiv.). After the addition of 35 mL of dry toluene, the suspension was heated to 95 °C for 16 h. In the next step the mixture was cooled to room temperature and filtered through Celite. The solvent of the filtrate was evaporated, and the crude product was purified by column chromatography on aluminum oxide (ethyl acetate/triethylamine 1 : 0.05). The volatiles were removed *in vacuo*, and the obtained tan oil was extracted with hexane and diethyl ether. Drying under vacuum yielded the product as a light brown solid (200 mg, 0.35 mmol, 21%). Single crystals suitable for X-ray diffraction analysis were grown by the slow evaporation of a concentrated solution of L^1 in acetonitrile. ^{1}H NMR (400.1 MHz, CD_2Cl_2): δ = 8.53–8.48 (m, 2H, 2 × CH^{Py}), 7.68–7.60 (m, 2H, 2 × CH^{Py}), 7.48–7.43 (m, 2H, 2 × CH^{Py}), 7.43–7.38 (m, 1H, CH^{Ar}), 7.30–7.24 (m, 1H, CH^{Ar}), 7.23–7.12 (m, 2H, 2 × CH^{Py}; 1H, CH^{Ar}), 7.11–7.03 (m, 1H, CH^{Ar}), 6.85–6.77 (m, 2H, 2 × CH^{Ar}), 4.93 (s, 4H, 2 × C$H_2{}^{Py}$), 3.76–3.65 (m, 4H, 2 × C$H_2{}^{Tacn}$), 2.79–2.65 (m, 4H, 2 × C$H_2{}^{Tacn}$; 2H, 2 × CH^{Tacn}), 2.43 (s, 4H, 2 × C$H_2{}^{Tacn}$), 0.86 ppm (d, ^3J(H,H) = 7 Hz, 12H, 4 × C$H_3{}^{Tacn}$); ^{13}C NMR (100.6 MHz, CD_2Cl_2): δ = 159.6 (2 × C^{Py}), 149.7 (2 × CH^{Py}), 146.1 (C^{Ar}), 145.7 (C^{Ar}), 136.8 (2 × CH^{Py}), 136.6 (C^{Ar}), 136.0 (C^{Ar}), 126.6 (C^{Ar}), 125.8 (C^{Ar}), 124.0 (CH^{Ar}), 123.6 (CH^{Ar}), 122.3 (2 × CH^{Py}), 122.0 (2 × CH^{Py}), 114.6 (CH^{Ar}), 113.4 (CH^{Ar}), 111.7 (CH^{Ar}), 108.6 (CH^{Ar}), 57.9 (2 × C$H_2{}^{Py}$), 54.6 (2 × CH^{Tacn}), 54.4 (2 × C$H_2{}^{Tacn}$), 53.3 (2 × C$H_2{}^{Tacn}$), 51.8 (2 × C$H_2{}^{Tacn}$), 18.4 ppm (4 × C$H_3{}^{Tacn}$); IR (KBr): $\tilde{\nu}$ = 2960 (m), 2929 (w), 2890 (w), 2793 (w), 1616 (m), 1591 (s), 1569 (w), 1499 (m), 1468 (w), 1460 (w), 1425 (s), 1395 (m), 1385 (m), 1355 (m), 1290 (w), 1249 (w), 1184 (m), 1164 (s), 1113 (w), 1083 (w), 1012 (w), 993 (w), 975 (w), 756 (s), 720 (m), 618 (w) cm^{-1}. ESI-MS (CH_3CN): m/z = 577.3661 (calcd for $[(L^1) + H]^+$: 577.3649), 599.3499 (calcd for $[(L^1) + Na]^+$: 599.3469); elemental analysis calcd (%) for $C_{36}H_{44}N_6O\cdot(C_4H_8O_2)_{0.5}$: C 73.52, H 7.79, N 13.54; found: C 73.20, H 7.97, N 13.07.

$iPr_2TacnHCH_2BF_3$: To a suspension of potassium (bromomethyl)trifluoroborate (1.5 g, 7.47 mmol) in dry thf (10 mL) was added iPr_2TacnH (1.86 mL, 7.8 mmol, 1.05 equiv.), and the mixture was heated to reflux for 5 h. After cooling to room temperature, the suspension was filtered through Celite and washed with acetone. Evaporation of the solvent yielded a brownish oil that was extracted with hexane and diethyl ether. After drying under vacuum, the product was obtained as a tan solid (730 mg, 2.47 mmol, 33%). ^{1}H NMR (400.1 MHz, $CDCl_3$): δ = 9.35 (s, 1H, NH), 3.35–3.28 (m, 2H, CH_2^{Tacn}), 3.05–2.95 (m, 2H, CH_2^{Tacn}), 2.94 (sept, $^3J_{H,H}$ = 7 Hz, 2H, 2 × CH), 2.88–2.79 (m, 2H, CH_2^{Tacn}), 2.74–2.66 (m, 2H, CH_2^{Tacn}), 2.58–2.52 (m, 2H, CH_2^{Tacn}), 2.36–2.28 (m, 2H, CH_2^{Tacn}), 2.22 (ps-d, 2H, CH_2BF_3), 1.07 (d, $^3J_{H,H}$ = 7 Hz, 6H, 2 × CH_3), 1.06 ppm (d, $^3J_{H,H}$ = 7 Hz, 6H, 2 × CH_3); ^{13}C NMR (100.6 MHz, $CDCl_3$): δ = 53.4 (2 × CH_2^{Tacn}), 52.1 (2 × CH^{Tacn}), 47.8 (2 × CH_2BF_3) 45.7 (2 × CH_2^{Tacn}), 42.6 (2 × CH_2^{Tacn}), 18.8 (2 × CH_3), 18.6 ppm (2 × CH_3); ^{19}F NMR (282.4 MHz, $CDCl_3$): δ = −142.1 ppm; IR (KBr): $\tilde{\nu}$ = 2962 (vs), 2930 (s), 2907 (s), 2870 (s), 2831 (s), 2806 (s), 1493 (s), 1466 (s), 1393 (s), 1370 (s), 1363 (m), 1318 (m), 1298 (s), 1280 (m), 1234 (m), 1197 (s), 1182 (s), 1170 (s), 1143 (m), 1121 (s), 1093 (vs), 1069 (vs), 1043 (vs), 1021 (vs), 1008 (vs), 996 (vs), 973 (vs), 906 (m), 845 (w), 798 (m), 770 (m), 736 (m), 712 (m), 577 (m), 533 (m), 493 (w) cm^{-1}; ESI-MS (CH_3CN): m/z = 317.2305 (calcd for $[(iPr_2TacnHCH_2BF_3) + Na]^+$: 317.2335), 333.2046 (calcd for $[(iPr_2TacnHCH_2BF_3) + K]^+$: 333.2075); elemental analysis calcd (%) for $C_{13}H_{19}N_3BF_3$: C 52.89, H 9.90, N 14.23; found: C 53.23, H 9.96, N 13.92.

L^2: A mixture of DBF-BrNPy$_2$ (582 mg, 1.31 mmol), $iPr_2TacnHCH_2BF_3$ (465 mg, 1.57 mmol, 1.2 equiv.), $Pd(OAc)_2$ (22 mg, 0.10 mmol, 0.075 equiv.), DavePhos (77 mg, 0.20 mmol, 0.15 equiv.) and caesium carbonate (1.28 g, 3.94 mmol, 3 equiv.) was suspended in dry toluene (35 mL) and heated to 97 °C for 18 h. The mixture was then cooled to room temperature and filtered through Celite. After the solvent of the filtrate was evaporated, the crude product was purified by column chromatography on aluminum oxide (hexane/ethyl acetate/triethylamine 1 : 1 : 0.05 → methanol). In the next step the obtained solid was extracted with ethyl acetate (10 × 30 mL). The combined ethyl acetate phases were filtered and

the solvent was removed *in vacuo* yielding a yellow oil. The latter was dissolved in 10 mL dichloromethane and extracted with 1 M NaOH. After the removal of the organic phase the aqueous phase was extracted with dichloromethane and the organic phases were combined and dried with $MgSO_4$. The solvent was removed, which thereby yielded the product as a yellow oil (477 mg, 0.81 mmol, 62%). ^{1}H NMR (400.1 MHz, CD_3CN): δ = 8.52–8.47 (m, 2H, 2 × CH^{Py}), 7.83–7.77 (m, 1H, CH^{Ar}), 7.63–7.57 (m, 2H, 2 × CH^{Py}), 7.51–7.44 (m, 3H, CH^{Ar}, 2 × CH^{Py}), 7.41–7.36 (m, 1H, CH^{Ar}), 7.29–7.23 (m, 1H, CH^{Ar}), 7.19–7.12 (m, 2H, 2 × CH^{Py}), 7.10–7.03 (m, 1H, CH^{Ar}), 6.82–6.77 (m, 1H, CH^{Ar}), 4.94 (s, 4H, 2 × C$H_2{}^{Py}$), 3.79 (s, 2H, CH_2), 2.84–2.77 (m, 4H, 2 × C$H_2{}^{Tacn}$), 2.75 (sept, $^3J_{H,H}$ = 6 Hz, 2H, 2 × CH^{Tacn}), 2.56–2.43 (m, 8H, 4 × C$H_2{}^{Tacn}$), 0.87 ppm (d, $^3J_{H,H}$ = 6 Hz, 12H, 4 × C$H_3{}^{Tacn}$); ^{13}C NMR (100.6 MHz, CD_3CN): δ = 160.3 (2 × C^{Py}), 155.1 (C^{Ar}), 150.1 (2 × CH^{Py}), 146.9 (C^{Ar}), 137.4 (2 × CH^{Py}), 136.8 (C^{Ar}), 128.8 (CH^{Ar}), 126.4 (C^{Ar}), 125.6 (C^{Ar}), 124.9 (C^{Ar}), 124.5 (CH^{Ar}), 123.6 (CH^{Ar}), 123.0 (2 × CH^{Py}), 122.7 (2 × CH^{Py}), 119.9 (CH^{Ar}), 115.1 (CH^{Ar}), 112.1 (CH^{Ar}), 58.8 (2 × C$H_2{}^{Py}$), 56.1 (1 × CH_2, 2 × C$H_2{}^{Tacn}$), 55.4 (2 × CH^{Tacn}), 53.51 (2 × C$H_2{}^{Tacn}$), 53.48 (2 × C$H_2{}^{Tacn}$), 18.6 ppm (4 × C$H_3{}^{Tacn}$); IR (ATR): $\tilde{\nu}$ = 3061 (s), 2960 (m), 2925 (m), 2867 (m), 1672 (w), 1590 (m), 1570 (w), 1504 (m), 1462 (m), 1431 (m), 1418 (m), 1381 (m), 1357 (m), 1306 (w), 1263 (w), 1183 (s), 1115 (w), 1093 (w), 1047 (w), 1032 (w), 994 (w), 947 (w), 862 (w), 758 (m), 728 (w), 618 (w), 578 (w) cm^{-1}; ESI-MS (CH_3CN): *m*/*z* = 591.3801 (calcd for [($\mathbf{L^2}$) + H]$^+$: 591.3806).

DBFTacnH: A Schlenk flask was charged with 4,6-dibromodibenzofuran (1 g, 3.07 mmol), TacnH (1.49 mL, 6.29 mmol, 2.05 equiv.), $Pd_2(dba)_3$ (140 mg, 0.15 mmol, 0.05 equiv.), DavePhos (121 mg, 0.31 mmol, 0.1 equiv.) and sodium *tert*-butoxide (443 mg, 4.61 mmol, 1.5 equiv.). After the addition of 20 mL of dry toluene, the suspension was heated to 95 °C for 24 h. The mixture was cooled to room temperature and filtered through Celite. The solvent of the filtrate was evaporated, and the crude product was purified by column chromatography on aluminum oxide (hexane/ethyl acetate/triethylamine 2 : 3 : 0.05). The volatiles were removed *in vacuo*. Drying under vacuum yielded the product as a light-yellow oil (65 mg, 0.17 mmol, 6%). ^{1}H NMR (400.1 MHz, CD_3CN): δ = 8.01–7.95 (m, 1H, CH^{Ar}), 7.59–7.54 (m, 1H, CH^{Ar}), 7.49–7.43 (m, 1H, CH^{Ar}), 7.39–7.32 (m, 2H, 2 × CH^{Ar}), 7.22–7.15 (m, 1H, CH^{Ar}), 6.90–6.83 (m, 1H, CH^{Ar}), 3.89–3.75 (m, 4H, 2 × C$H_2{}^{Tacn}$), 2.91–2.79 (m, 6H, 2 × C$H_2{}^{Tacn}$, 2 × CH^{Tacn}), 2.53 (s, 4H, 2 × C$H_2{}^{Tacn}$), 0.88 ppm (d, ^3J(H,H) = 7 Hz, 12H, 4 × C$H_3{}^{Tacn}$); ^{13}C NMR (75.5 MHz, CD_3CN): δ = 156.1 (C^{Ar}), 146.9 (C^{Ar}), 137.0 (C^{Ar}), 127.8 (CH^{Ar}), 125.9 (C^{Ar}), 125.5 (C^{Ar}), 124.8 (CH^{Ar}), 123.6 (CH^{Ar}), 121.6 (CH^{Ar}), 114.3 (CH^{Ar}), 112.4 (CH^{Ar}), 110.0 (CH^{Ar}), 54.9 (2 × CH^{Tacn}), 54.4 (2 × C$H_2{}^{Tacn}$), 53.1 (2 × C$H_2{}^{Tacn}$), 51.8 (2 × C$H_2{}^{Tacn}$), 18.4 ppm (4 × C$H_3{}^{Tacn}$). IR (ATR): $\tilde{\nu}$ = 3061 (m), 2959 (w), 2925 (w), 2867 (w), 3021 (w), 1672 (w), 1624 (m), 1504 (m), 1450 (m), 1421 (w), 1380 (w), 1359 (m), 1351 (m), 1322 (w), 1295 (w), 1262 (w), 1245 (w), 1185 (m), 1163 (s), 1115 (w), 1090 (w), 1077 (w), 999 (w), 989 (w), 926 (w), 830 (w), 780 (w), 739 (s), 639 (w), 571 (w), 562 (w) cm^{-1}. ESI-MS (CH_3CN): *m*/*z* = 380.2758 (calcd for [(DBF-HTacn) + H]$^+$: 380.2696).

Complex synthesis

[($\mathbf{L^1}$)(CuCl)$_2$] (1). $\mathbf{L^1}$ (19 mg, 32.9 μmol) and CuCl (6.5 mg, 65.9 μmol, 2 equiv.) were dissolved in acetonitrile (3 mL) and stirred for 6 h. In the next step the volume of the resulting solution was reduced under vacuum to 1 mL. The addition of diethyl ether (20 mL) caused the precipitation of a yellow solid that was collected by filtration, washed with hexane, and dried under vacuum to yield **1** (19.3 mg, 24.9 μmol, 76%). Single crystals suitable for X-ray diffraction analysis were grown by slow diffusion of diethyl ether into a concentrated solution of **1** in acetone. ^{1}H NMR (500.1 MHz, CD_2Cl_2): δ = 8.94–8.78 (br., 2H, 2 × CH^{Py}), 8.57–8.11 (br., 1H, CH^{Ar}), 7.96–7.78 (m, br., 2H, 2 × CH^{Py}), 7.78–7.64 (br., 1H, CH^{Ar}), 7.64–7.43 (m, 3H, CH^{Ar}, 2 × CH^{Py}), 7.43–7.30 (br., 2H, 2 × CH^{Py}), 7.30–7.19 (m, br., 1H, CH^{Ar}), 7.18–7.03 (m, br., 2H, 2 × CH^{Ar}), 4.69 (s, 4H, 2 × C$H_2{}^{Py}$), 3.47–3.07 (m, br., 6H, 2 × C$H_2{}^{Tacn}$, 2 × CH^{Tacn}), 2.92–2.63 (m, br., 4H, 2 × C$H_2{}^{Tacn}$), 2.59–2.24 (m, br., 4H, 2 × C$H_2{}^{Tacn}$), 1.22 ppm (br., 12H, 4 × C$H_3{}^{Tacn}$); IR (ATR): $\tilde{\nu}$ = 2964 (w), 2924 (w), 2849 (w), 1619 (w), 1600 (m), 1568 (w), 1495 (w), 1433 (m), 1414 (w), 1387 (w), 1367 (w), 1336 (w), 1272 (w) 1239 (w), 1185 (m), 1153 (m), 1123 (w), 1097 (w), 1071 (w), 1055 (w), 1017 (w), 980 (w), 961 (w), 937 (w), 900 (w), 866 (w), 842 (w), 820 (w), 771 (s), 733 (w), 690 (w), 636 (w), 569 (w), 553 (w), 515 (w), 465 (w), 452 (w) cm^{-1}; ESI-MS (CH_3CN): *m*/*z* = 351.1100 (calcd for [($\mathbf{L^1}$)(Cu)$_2$]$^{2+}$: 351.1079), 639.2891 (calcd for [($\mathbf{L^1}$)(Cu)]$^+$: 639.2867), 737.1784 (calcd for [($\mathbf{L^1}$)(Cu)$_2$Cl]$^+$: 737.1852), 773.1499 (calcd for [($\mathbf{L^1}$)(CuCl)$_2$ + H]$^+$: 773.1618).

[(($\mathbf{L^1}$)(CuBr)$_2$)$_2$(μ-(Cu$_2$)(μ-Br)$_2$)] (2). A yellow solution of $\mathbf{L^1}$ (33 mg, 57.2 μmol) and CuBr (24.6 mg, 171.6 μmol, 3 equiv.) in acetonitrile (6 mL) was stirred for 6 h at room temperature. The product was isolated by following the same procedure as that described above for complex **1**. After work-up, **2** (36 mg, 35.7 μmol, 62%) was obtained as a yellow solid. Single crystals suitable for X-ray diffraction analysis were grown by slow diffusion of diethyl ether into a concentrated solution of **2** in acetone. ^{1}H NMR (300.1 MHz, CD_3CN): δ = 8.75–8.66 (m, 2H, 2 × CH^{Py}), 7.98–7.77 (m, 3H, 2 × CH^{Py}, CH^{Ar}), 7.63–7.53 (m, 3H, 2 × CH^{Py}, CH^{Ar}), 7.48–7.38 (m, 2H, 2 × CH^{Py}), 7.33–7.22 (m, 1H, CH^{Ar}), 7.18–6.97 (m, br., 3H, 3 × CH^{Ar}), 4.77 (s, 4H, 2 × C$H_2{}^{Py}$), 3.38–2.89 (m, br., 6H, 2 × CH^{Tacn}, 2 × C$H_2{}^{Tacn}$), 2.89–2.58 (m, br., 2 × C$H_2{}^{Tacn}$), 2.56–2.12 (m, br., 2 × C$H_2{}^{Tacn}$), 1.20 ppm (br., 12H, 4 × C$H_3{}^{Tacn}$); IR (ATR): $\tilde{\nu}$ = 2962 (w), 2926 (w), 2852 (w), 1671 (w), 1599 (m), 1568 (w), 1495 (w), 1479 (w), 1432 (m), 1412 (w), 1386 (w), 1367 (w), 1337 (w), 1261 (m), 1184 (w), 1175 (w), 1153 (m), 1119 (m), 1097 (m), 1073 (m), 1053 (m), 1019 (s), 981 (w), 962 (w), 938 (w), 870 (w), 845 (w), 818 (w), 800 (s), 775 (s), 736 (w), 597 (w), 516 (w) cm^{-1}; ESI-MS (acetone): *m*/*z* = 639.2850 (calcd for [($\mathbf{L^1}$)(Cu)]$^+$: 639.2867), 719.2047 (calcd for [($\mathbf{L^1}$)(CuBr) + H]$^+$: 719.2129), 781.1302 (calcd for [($\mathbf{L^1}$)(Cu)$_2$Br]$^+$: 781.1347); elemental analysis (%) for $C_{72}H_{88}N_{12}O_2Cu_6Br_6$: C 42.94, H 4.40, N 8.34; found C 43.40, H 4.47, N 8.44.

[(($\mathbf{L^1}$)(CuI)$_2$)$_2$(μ-(Cu$_2$)(μ-I)$_2$)] (3). A yellow solution of $\mathbf{L^1}$ (40 mg, 69.4 μmol) and CuI (39.6 mg, 208.1 μmol, 3 equiv.) in acetonitrile (6 mL) was stirred for 6 h at room temperature. The product was isolated by following the same procedure as

that described above for complex **1**. After work-up, **3** (37 mg, 32.2 μmol, 46%) was obtained as a yellow solid. Single crystals suitable for X-ray diffraction analysis were grown by slow evaporation of a concentrated solution of **3** in acetonitrile. ^{1}H NMR (300.1 MHz, CD_2Cl_2): δ = 9.05–8.84 (m, 2H, 2 × CH^{Py}), 8.50–8.26 (br., 1H, CH^{Ar}), 7.88–7.77 (m, 2H, 2 × CH^{Py}), 7.77–7.67 (br., 1H, CH^{Ar}), 7.61–7.53 (m, 1H, CH^{Ar}), 7.52–7.43 (br., 2H, 2 × CH^{Py}), 7.42–7.35 (m, 2H, 2 × CH^{Py}), 7.26–7.18 (m, 1H, CH^{Ar}), 7.17–7.10 (m, 1H, CH^{Ar}), 7.09–6.99 (br., 1H, CH^{Ar}), 4.68 (s, 4H, 2 × C$H_2{}^{Py}$), 3.47–3.04 (br., 6H, 2 × C$H_2{}^{Tacn}$, 2 × CH^{Tacn}), 2.88–2.61 (br., 4H, 2 × C$H_2{}^{Tacn}$), 2.58–2.26 (br., 4H, 2 × C$H_2{}^{Tacn}$), 1.22 ppm (br., 12H, 4 × C$H_3{}^{Tacn}$); IR (ATR): $\tilde{\nu}$ = 2963 (w), 2925 (w), 2849 (w), 1671 (w), 1618 (w), 1598 (m), 1568 (w), 1495 (w), 1479 (w), 1432 (m), 1414 (w), 1385 (w), 1367 (w), 1335 (w), 1270 (w) 1239 (w), 1185 (w), 1152 (m), 1121 (w), 1098 (w), 1069 (w), 1053 (w), 1016 (w), 981 (w), 962 (w), 937 (w), 866 (w), 844 (w), 820 (w), 769 (s), 735 (m), 689 (w), 575 (w), 514 (w), 464 (w), 416 (w) cm^{-1}; ESI-MS (CH_3CN): m/z = 351.1099 (calcd for $[(\mathbf{L^1})(Cu)_2]^{2+}$: 351.1079), 639.2915 (calcd for $[(\mathbf{L^1})(Cu)]^+$: 639.2867), 767.2034 (calcd for $[(\mathbf{L^1})(CuI) + H]^+$: 767.1990), 829.1253 (calcd for $[(\mathbf{L^1})(Cu)_2I]^+$: 829.1208), 957.0343 (calcd for $[(\mathbf{L^1})(CuI)_2 + H]^+$: 957.0331); elemental analysis (%) for $C_{72}H_{88}N_{12}O_2Cu_6I_6\cdot(C_4H_{10}O)$: C 38.51, H 4.17, N 7.09; found C 38.48, H 3.83, N 7.20.

$[(\mathbf{L^1})(Cu(NCCH_3))_2](BF_4)_2$ (4). $\mathbf{L^1}$ (53.3 mg, 92.4 μmol) and $[Cu(NCCH_3)]BF_4$ (58.1 mg, 184.8 μmol, 2 equiv.) were dissolved in acetonitrile (5 mL) and stirred for 6 h at room temperature. The product was isolated by following the same procedure as that described for complex **1**. After work-up **4** (59.3 mg, 61.8 μmol, 67%) was obtained. Single crystals suitable for X-ray diffraction analysis were obtained by slow diffusion of diethyl ether into a concentrated solution of **4** in acetonitrile. ^{1}H NMR (400.1 MHz, CD_3CN): δ = 8.65–8.55 (m, 2H, 2 × CH^{Py}), 8.03–7.95 (m, 2H, 2 × CH^{Py}), 7.94–7.91 (m, 1H, CH^{Ar}), 7.74–7.66 (m, 2H, 2 × CH^{Ar}), 7.66–7.61 (m, 2H, 2 × CH^{Py}), 7.54–7.47 (m, 2H, 2 × CH^{Py}), 7.41–7.35 (m, 1H, CH^{Ar}), 7.23–7.17 (m, 1H, CH^{Ar}), 7.13–7.08 (m, 1H, CH^{Ar}), 4.82 (s, 4H, 2 × C$H_2{}^{Py}$), 3.20–3.06 (m, 4H, 2 × CH^{Tacn}, C$H_2{}^{Tacn}$), 3.04–2.93 (m, 2H, C$H_2{}^{Tacn}$), 2.92–2.79 (m, 2H, C$H_2{}^{Tacn}$), 2.76–2.63 (m, 2H, C$H_2{}^{Tacn}$), 2.53–2.42 (m, 2H, C$H_2{}^{Tacn}$), 2.38–2.27 (m, 2H, C$H_2{}^{Tacn}$), 1.96 (s, 6H, 2 × NCCH_3), 1.24 (d, $^3J_{H,H}$ = 7 Hz, 6H, 2 × C$H_3{}^{Tacn}$), 1.20 ppm (d, ^3J(H,H) = 7 Hz, 6H, 2 × C$H_3{}^{Tacn}$); ^{13}C NMR (75.5 MHz, CD_3CN): δ = 157.2 (2 × C^{Py}), 150.3 (2 × CH^{Py}), 150.2 (C^{Ar}), 147.8 (C^{Ar}), 139.6 (2 × CH^{Py}), 138.1 (C^{Ar}), 135.4 (C^{Ar}), 127.7 (C^{Ar}), 126.8 (CH^{Ar}), 126.1 (C^{Ar}), 125.47 (2 × CH^{Py}), 125.44 (2 × CH^{Py}), 124.9 (2 × CH^{Ar}), 120.3 (CH^{Ar}), 116.3 (CH^{Ar}), 116.0 (CH^{Ar}), 58.9 (2 × CH^{Tacn}), 58.6 (2 × C$H_2{}^{Py}$), 56.2 (2 × C$H_2{}^{Tacn}$), 51.2 (4 × C$H_2{}^{Tacn}$), 20.2 (2 × C$H_3{}^{Tacn}$), 19.8 ppm (2 × C$H_3{}^{Tacn}$); ^{19}F NMR (282.4 MHz, CD_3CN): δ = −150.51 ppm; IR (ATR): $\tilde{\nu}$ = 2972 (w), 2935 (w), 2870 (w), 2853 (w), 2260 (w), 1678 (w), 1602 (w), 1496 (w), 1484 (w), 1435 (w), 1415 (w), 1390 (w), 1370 (w), 1186 (w), 1150 (w), 1049 (s), 1034 (s), 983 (m), 965 (w), 937 (w), 844 (w), 774 (m), 738 (w), 520 (w) cm^{-1}. ESI-MS (CH_3CN): m/z = 351.1125 (calcd for $[(\mathbf{L^1})(Cu)_2]^{2+}$: 351.1079), 371.6278 (calcd for $[(\mathbf{L^1})(Cu)_2(NCCH_3)]^{2+}$: 371.6212), 577.3634 (calcd for $[\mathbf{L^1}]^+$: 577.3649), 639.2903 (calcd for $[(\mathbf{L^1})(Cu)]^+$: 639.2867), 721.2068 (calcd for $[(\mathbf{L^1})(Cu)_2F]^+$: 721.2147); elemental analysis (%) for $C_{40}H_{50}N_8OCu_2B_2F_8$: C 50.07, H 5.25, N 11.68; found C 50.17, H 5.46, N 11.66.

$[(\mathbf{L^1})(Cu(NCCH_3))(Cu(OTf))](OTf)$ (5). A solution of $\mathbf{L^1}$ (46.6 mg, 80.8 μmol) and $[Cu(NCCH_3)_4]OTf$ (60.9 mg, 161.6 μmol, 2 equiv.) in acetonitrile (7 mL) was stirred for 6 h at room temperature. The isolation of the product was accomplished following the same procedure as that described for **1**. After work-up **5** was isolated as a yellow solid (57 mg, 54.6 μmol, 68%). ^{1}H NMR (400.1 MHz, CD_3CN): δ = 8.67–8.60 (m, 2H, 2 × CH^{Py}), 8.04–7.97 (m, 2H, 2 × CH^{Py}), 7.95–7.90 (m, 1H, CH^{Ar}), 7.76–7.60 (m, 4H, 2 × CH^{Ar}, 2 × CH^{Py}), 7.57–7.47 (m, 2H, 2 × CH^{Py}), 7.44–7.35 (m, 1H, CH^{Ar}), 7.27–7.17 (m, 1H, CH^{Ar}), 7.16–7.08 (m, 1H, CH^{Ar}), 4.83 (s, 4H, 2 × C$H_2{}^{Py}$), 3.20–3.09 (m, 4H, 2 × CH^{Tacn}; C$H_2{}^{Tacn}$), 3.04–2.95 (m, 2H, C$H_2{}^{Tacn}$), 2.91–2.81 (m, 2H, C$H_2{}^{Tacn}$), 2.75–2.65 (m, 2H, C$H_2{}^{Tacn}$), 2.56–2.44 (m, 2H, C$H_2{}^{Tacn}$), 2.39–2.28 (m, 2H, C$H_2{}^{Tacn}$), 1.96 (s, 3H, 1 × NCCH_3), 1.24 (d, $^3J_{H,H}$ = 7 Hz, 6H, 2 × C$H_3{}^{Tacn}$), 1.20 ppm (d, $^3J_{H,H}$ = 7 Hz, 6H, 2 × C$H_3{}^{Tacn}$); ^{13}C NMR (100.6 MHz, CD_3CN): δ = 157.3 (2 × C^{Py}), 150.33 (2 × CH^{Py}), 150.26 (C^{Ar}), 147.8 (C^{Ar}), 139.5 (2 × CH^{Py}), 138.1 (C^{Ar}), 135.4 (C^{Ar}), 127.7 (C^{Ar}), 126.8 (CH^{Ar}), 126.1 (C^{Ar}), 125.45 (2 × CH^{Py}), 125.43 (2 × CH^{Py}), 124.93 (CH^{Ar}), 124.91 (CH^{Ar}), 120.3 (CH^{Ar}), 116.3 (CH^{Ar}), 116.0 (CH^{Ar}), 58.9 (2 × CH^{Tacn}), 58.6 (2 × C$H_2{}^{Py}$), 56.2 (2 × C$H_2{}^{Tacn}$), 51.3 (4 × C$H_2{}^{Tacn}$), 20.2 (2 × C$H_3{}^{Tacn}$), 19.8 (2 × C$H_3{}^{Tacn}$). ^{19}F NMR (282.4 MHz, CD_3CN): δ = −78.22 ppm; IR (KBr): $\tilde{\nu}$ = 2973 (w), 2933 (w), 2872 (w), 1602 (w), 1496 (m), 1435 (w), 1416 (w), 1387 (w), 1369 (w), 1266 (s), 1238 (m), 1222 (m), 1152 (m), 1030 (s), 776 (m), 637 (s), 573 (w), 517 (w) cm^{-1}; ESI-MS (CH_3CN): m/z = 351.1113 (calcd for $[(\mathbf{L^1})(Cu)_2]^{2+}$: 351.1079), 371.6248 (calcd for $[(\mathbf{L^1})(Cu)_2(NCCH_3)]^{2+}$: 371.6212), 577.3634 (calcd for $[\mathbf{L^1}]^+$: 577.3649), 639.2931 (calcd for $[(\mathbf{L^1})(Cu)]^+$: 639.2867), 789.2534 (calcd for $[(\mathbf{L^1})((Cu)OTf) + H]^+$: 789.2466), 851.1755 (calcd for $[(\mathbf{L^1})(Cu)_2OTf]^+$: 851.1683); elemental analysis (%) for $C_{40}H_{47}N_7O_7Cu_2F_6S_2$: C 46.06, H 4.54, N 9.40; found C 46.58, H 4.70, N 9.58.

$[(\mathbf{L^1})(Cu(NCCH_3))(Cu(ClO_4))](ClO_4)$ (6). $\mathbf{L^1}$ (52 mg, 90.2 μmol) and $[Cu(NCCH_3)_4]ClO_4$ (59 mg, 180.4 μmol, 2 equiv.) were dissolved in acetonitrile (5 mL) and the resulting solution was stirred at room temperature for 6 h. The product was isolated following the same procedure as that described for complex **1**. After work-up **6** was obtained as a yellow solid (60.7 mg, 61.4 μmol, 68%). Single crystals suitable for X-ray diffraction analysis were obtained by slow diffusion of diethyl ether into a concentrated solution of **4** in acetone. ^{1}H NMR (400.1 MHz, CD_3CN): δ = 8.66–8.59 (m, 2H, 2 × CH^{Py}), 8.03–7.96 (m, 2H, 2 × CH^{Py}), 7.96–7.90 (m, 1H, CH^{Ar}), 7.77–7.60 (m, 4H, 2 × CHAr, 2 × CH^{Py}), 7.55–7.47 (m, 2H, 2 × CH^{Py}), 7.41–7.34 (m, 1H, CH^{Ar}), 7.24–7.16 (m, 1H, CH^{Ar}), 7.15–7.07 (m, 1H, CH^{Ar}), 4.82 (s, 4H, 2 × C$H_2{}^{Py}$), 3.20–3.07 (m, 2H, 2 × CH^{Tacn}; 2H, C$H_2{}^{Tacn}$), 3.03–2.94 (m, 2H, C$H_2{}^{Tacn}$), 2.91–2.81 (m, 2H, C$H_2{}^{Tacn}$), 2.75–2.66 (m, 2H, C$H_2{}^{Tacn}$), 2.54–2.45 (m, 2H, C$H_2{}^{Tacn}$), 2.38–2.29 (m, 2H, C$H_2{}^{Tacn}$), 1.96 (s, 3H, 1 × NCCH_3), 1.24 (d, $^3J_{H,H}$ = 7 Hz, 6H, 2 × C$H_3{}^{Tacn}$), 1.20 ppm (d, $^3J_{H,H}$ = 7 Hz, 6H, 2 × C$H_3{}^{Tacn}$); ^{13}C NMR (75.5 MHz, CD_3CN): δ = 157.2 (2 × C^{Py}), 150.3 (2 × CH^{Py}), 150.2 (C^{Ar}), 147.8 (C^{Ar}), 139.5 (2 × CH^{Py}),

138.1 (C^{Ar}), 135.4 (C^{Ar}), 127.6 (C^{Ar}), 126.8 (CH^{Ar}), 126.1 (C^{Ar}), 125.4 (4 × CH^{Py}), 124.9 (CH^{Ar}), 124.8 (CH^{Ar}), 120.2 (CH^{Ar}), 116.2 (CH^{Ar}), 115.9 (CH^{Ar}), 58.9 (2 × CH^{Tacn}), 58.6 (2 × CH_2^{Py}), 56.2 (2 × CH_2^{Tacn}), 51.2 (4 × CH_2^{Tacn}), 20.2 (2 × CH_3^{Tacn}), 19.8 ppm (2 × CH_3^{Tacn}); IR (ATR): $\tilde{\nu}$ = 2972 (w), 2932 (w), 1657 (w), 1600 (w), 1495 (w), 1483 (w), 1434 (w), 1414 (w), 1389 (w), 1368 (w), 1183 (w), 1091 (s), 982 (w), 963 (w), 933 (w), 866 (w), 843 (w), 820 (w), 775 (w), 623 (m) cm^{-1}; ESI-MS (CH_3CN): m/z = 351.1082 (calcd for $[(\mathbf{L^1})(Cu)_2]^{2+}$: 351.1079), 371.6215 (calcd for $[(\mathbf{L^1})(Cu)_2(NCCH_3)]^{2+}$: 371.6212), 639.2868 (calcd for $[(\mathbf{L^1})(Cu)]^+$: 639.2867), 737.1858 (calcd for $[(\mathbf{L^1})(Cu)_2Cl]^+$: 737.1852), 801.1644 (calcd for $[(\mathbf{L^1})(Cu)_2(ClO_4)]^+$: 801.1648); elemental analysis (%) for $C_{38}H_{47}N_7O_9Cu_2Cl_2$: C 48.36, H 5.02, N 10.39; found C 48.68, H 5.26, N 10.92.

$[(\mathbf{L^1})(Cu_2(dppe))](PF_6)$ (7). $\mathbf{L^1}$ (22 mg, 38.1 μmol) and $[Cu(NCCH_3)_4]PF_6$ (28.4 mg, 76.2 μmol, 2 equiv.) were dissolved in acetone (3 mL). After stirring for 7 h at room temperature, 1,2-bis(diphenylphosphino)ethane (15.2 mg, 38.1 μmol, 1 equiv.) dissolved in acetone (1 mL) was added and the reaction mixture was left to stir for another 15 h. In the next step the volume of the solution was reduced under vacuum to 1 mL, followed by the addition of diethyl ether (20 mL) that caused the precipitation of a light yellow solid. This solid was isolated by filtration, washed with hexane and dried under vacuum. The desired product **7** was obtained as a light yellow solid (26 mg, 18.7 μmol, 49%). Diffusion of diethyl ether into a solution of **7** in acetonitrile provided light yellow crystals which were suitable for X-ray diffraction analysis. IR (KBr): $\tilde{\nu}$ = 2967 (w), 2932 (w), 2870 (w), 1603 (w), 1497 (w), 1483 (w), 1436 (w), 1417 (w), 1386 (w), 1369 (w), 1161 (w), 1144 (w), 1118 (w), 1100 (vs), 840 (s), 771 (w), 742 (w), 720 (w), 696 (w), 558 (m), 517 (w) cm^{-1}; ESI-MS (acetone): m/z = 550.1764 (calcd for $[(\mathbf{L^1})(Cu)_2(dppe)]^{2+}$: 550.1755), 639.2873 (calcd for $[(\mathbf{L^1})(Cu)]^+$: 639.2867), 1245.3170 (calcd for $[(\mathbf{L^1})(Cu)_2(dppe)(PF_6)]^+$: 1245.3158).

$\{[Cu_2(\mathbf{L^2})Cl_2]\}_n$, (8). A solution of $\mathbf{L^2}$ (24 mg, 40.6 μmol) and CuCl (8.1 mg, 81.2 μmol, 2 equiv.) in acetonitrile (3 mL) was stirred for 6 h. In the next step the volume of the resulting solution was reduced under vacuum to 1 mL, followed by the addition of diethyl ether (20 mL) that caused the precipitation of a yellow solid. This solid was collected by filtration, washed with hexane, and dried under vacuum to yield **8** (18.3 mg, 23.2 μmol, 57%). ^{1}H NMR (300.1 MHz, CD_3CN): δ = 8.69–8.61 (m, 2H, 2 × CH^{Py}), 8.04–7.95 (m, 1H, CH^{Ar}), 7.93–7.83 (m, 2H, 2 × CH^{Py}), 7.71–7.61 (m, 2H, 2 × CH^{Ar}), 7.61–7.51 (m, 2H, 2 × CH^{Ar}), 7.45–7.36 (m, 3H, CH^{Ar}, 2 × CH^{Py}),7.23–7.13 (m, 2H, 2 × CH^{Py}), 4.77 (s, 4H, 2 × CH_2^{Py}), 4.12 (s, 2H, CH_2), 2.88–2.74 (m, 4H, 2 × CH^{Tacn}, CH_2^{Tacn}), 2.74–2.61 (m, 2H, CH_2^{Tacn}), 2.59–2.29 (m, 8H, 4 × CH_2^{Tacn}), 1.08 (d, $^3J_{H,H}$ = 6.7 Hz, 6H, 2 × CH_3^{Tacn}), 1.03 ppm (d, $^3J_{H,H}$ = 6.4 Hz, 6H, 2 × CH_3^{Tacn}); ^{13}C NMR (75.5 MHz, CD_3CN): δ = 157.6 (2 × C^{Py}), 155.7 (C^{Ar}), 150.5 (2 × CH^{Py}), 148.4 (C^{Ar}), 138.9 (2 × CH^{Py}), 135.7 (C^{Ar}), 131.8 (CH^{Ar}), 126.7 (C^{Ar}), 125.1 (C^{Ar}), 125.0 (2 × CH^{Py}), 124.9 (2 × CH^{Py}), 124.6 (CH^{Ar}), 124.0 (CH^{Ar}), 122.1 (CH^{Ar}), 121.2 (C^{Ar}), 117.2 (CH^{Ar}), 115.6 (CH^{Ar}), 58.5 (2 × CH^{Tacn}), 58.3 (2 × CH_2^{Py}), 57.6 (CH_2), 54.7 (2 × CH_2^{Tacn}), 50.9 (2 × CH_2^{Tacn}), 50.3 (2 × CH_2^{Tacn}), 19.9 (2 × CH_3^{Tacn}), 19.5 ppm (2 × CH_3^{Tacn}); IR (ATR): $\tilde{\nu}$ = 3393 (w), 3325 (w), 3188 (w), 3058 (w), 3021 (w), 2966 (m), 2927 (m), 2846 (m), 1674 (s), 1600 (s), 1569 (w), 1495 (m), 1480 (m), 1434 (vs), 1418 (m), 1385 (m), 1367 (m), 1342 (w), 1294 (w), 1275 (w), 1249 (w), 1181 (s), 1155 (m), 1129 (m), 1101 (w), 1071 (w), 1052 (w), 1017 (w), 977 (w), 960 (w), 945 (w), 862 (w), 841 (w), 813 (w), 769 (vs), 737 (m), 577 (w), 508 (w), 410 (w) cm^{-1}; MS (ESI, CH_3CN): m/z = 358.1180 (calcd for $[(\mathbf{L^2})(Cu)_2]^{2+}$: 358.1157). 653.3091 (calcd for $[(\mathbf{L^2})(Cu)]^+$: 653.3024), 751.2092 (calcd for $[(\mathbf{L^2})(Cu)_2Cl]^+$: 751.2008).

$[(\mathbf{L^2})(Cu(NCCH_3))_2](PF_6)_2$ (9). $\mathbf{L^2}$ (46.5 mg, 78.7 μmol) and $[Cu(NCCH_3)_4]PF_6$ (58.7 mg, 157.4 μmol, 2 equiv.) were dissolved in acetonitrile (5 mL) and stirred for 4 h at room temperature. The product was isolated by following the same procedure as that described for complex **8**. After work-up **9** (43.5 mg, 39.9 μmol, 51%) was obtained. Single crystals suitable for X-ray diffraction analysis were obtained by slow diffusion of diethyl ether into a concentrated solution of **9** in acetonitrile. ^{1}H NMR (400.1 MHz, CD_3CN): δ = 8.64–8.59 (m, 2H, 2 × CH^{Py}), 8.07–8.02 (m, 1H, CH^{Ar}), 7.98–7.91 (m, 2H, 2 × CH^{Py}), 7.75–7.70 (m, 1H, CH^{Ar}), 7.70–7.66 (m, 1H, CH^{Ar}), 7.63–7.57 (m, 2H, 2 × CH^{Py}), 7.51–7.41 (m, 3H, CH^{Ar}, 2 × CH^{Py}), 7.25–7.20 (m, 2H, 2 × CH^{Ar}), 4.76 (s, 4H, 2 × CH_2^{Py}), 4.10 (s, 2H, CH_2), 2.89–2.74 (m, 4H, 2 × CH^{Tacn}, CH_2^{Tacn}), 2.75–2.63 (m, 2H, CH_2^{Tacn}), 2.52–2.38 (m, 6H, 3 × CH_2^{Tacn}), 2.38–2.26 (m, 2H, CH_2^{Tacn}), 1.96 (s, 6H, 2 × $NCCH_3$), 1.08 (d, $^3J_{H,H}$ = 6.4 Hz, 6H, 2 × CH_3^{Tacn}), 1.03 (d, $^3J_{H,H}$ = 6.8 Hz, 6H, 2 × CH_3Tacn) ppm; ^{13}C NMR (100.6 MHz, CD_3CN): δ = 157.2 (2 × C^{Py}), 155.6 (C^{Ar}), 150.4 (2 × CH^{Py}), 148.6 (C^{Ar}), 139.6 (2 × CH^{Py}), 135.2 (C^{Ar}), 131.9 (CH^{Ar}), 126.8 (C^{Ar}), 125.5 (4 × CH^{Py}), 125.2 (C^{Ar}), 124.8 (CH^{Ar}), 124.3 (CH^{Ar}), 122.4 (CH^{Ar}), 121.0 (C^{Ar}), 117.5 (CH^{Ar}), 116.7 (CH^{Ar}), 58.6 (2 × CH^{Tacn}), 58.3 (2 × CH_2^{Py}), 57.5 (CH_2), 54.8 (2 × CH_2^{Tacn}), 51.0 (2 × CH_2^{Tacn}), 50.2 (2 × CH_2^{Tacn}), 19.9 (2 × CH_3^{Tacn}), 19.5 ppm (2 × CH_3^{Tacn}); ^{31}P NMR (162.0 MHz, CD_3CN): δ = −143.28 ppm. ^{19}F NMR (282.4 MHz, CD_3CN): δ = −71.92 ppm. IR (ATR): $\tilde{\nu}$ = 2973 (w), 2938 (w), 2846 (w), 1675 (w), 1603 (w), 1495 (w), 1436 (w), 1418 (w), 1388 (w), 1370 (w), 1179 (w), 1130 (w), 1020 (w), 946 (w), 875 (w), 834 (s), 772 (m), 739 (w), 557 (s) cm^{-1}; ESI-MS (CH_3CN): m/z = 358.1225 (calcd for $[(\mathbf{L^2})(Cu)_2]^{2+}$: 358.1157), 653.3029 (calcd for $[(\mathbf{L^2})(Cu)]^+$: 653.3024); elemental analysis for $C_{41}H_{52}N_8OCu_2P_2F_{12}$: C 45.18, H 4.81, N 10.28; found C 45.65, H 4.97, N 10.16.

$[(\mathbf{L^2})(Cu(NCCH_3))_2](OTf)_2$ (10). A solution of $\mathbf{L^2}$ (46.8 mg, 79.2 μmol) and $[Cu(NCCH_3)_4]OTf$ (59.7 mg, 158.4 μmol, 2 equiv.) in acetonitrile (5 mL) was stirred at room temperature for 4 h. The product was isolated by following the same procedure as that described for complex **8**. After work-up **10** (47.6 mg, 43.3 μmol, 55%) was obtained. ^{1}H NMR (400.1 MHz, CD_3CN): δ = 8.65–8.60 (m, 2H, 2 × CH^{Py}), 8.07–8.03 (m, 1H, CH^{Ar}), 7.99–7.92 (m, 2H, 2 × CH^{Py}), 7.76–7.71 (m, 1H, CH^{Ar}), 7.71–7.66 (m, 1H, CH^{Ar}), 7.64–7.58 (m, 2H, 2 × CH^{Py}), 7.51–7.41 (m, 3H, CH^{Ar}, 2 × CH^{Py}), 7.25–7.21 (m, 2H, 2 × CH^{Ar}), 4.76 (s, 4H, 2 × CH_2^{Py}), 4.10 (s, 2H, CH_2), 2.88–2.74 (m, 4H, 2 × CH^{Tacn}, CH_2^{Tacn}), 2.74–2.62 (m, 2H, CH_2^{Tacn}), 2.50–2.39 (m, 6H, 3 × CH_2^{Tacn}), 2.38–2.29 (m, 2H, CH_2^{Tacn}), 1.96 (s, 6H, 2 × CH_3CN), 1.08 (d, $^3J_{H,H}$ = 7 Hz, 6H, 2 × CH_3^{Tacn}), 1.03 ppm (d, $^3J_{H,H}$ =

7 Hz, 6H, 2 × CH_3^{Tacn}); ^{13}C NMR (100.6 MHz, CD_3CN): δ = 157.2 (2 × C^{Py}), 155.6 (C^{Ar}), 150.4 (2 × CH^{Py}), 148.6 (C^{Ar}), 139.6 (2 × CH^{Py}), 135.2 (C^{Ar}), 131.9 (CH^{Ar}), 126.8 (C^{Ar}), 125.53 (2 × CH^{Py}), 125.51 (2 × CH^{Py}), 125.2 (C^{Ar}), 124.8 ($CHAr$), 124.3 (CH^{Ar}), 122.5 (CH^{Ar}), 121.0 (C^{Ar}), 117.5 (CH^{Ar}), 116.7 (CH^{Ar}), 58.6 (2 × CH^{Tacn}), 58.3 (2 × CH_2^{Py}), 57.4 (CH_2), 54.8 (2 × CH_2^{Tacn}), 51.0 (2 × CH_2^{Tacn}), 50.2 (2 × CH_2^{Tacn}), 19.9 (2 × CH_3^{Tacn}), 19.5 ppm (2 × CH_3^{Tacn}); IR (ATR): $\tilde{\nu}$ = 2976 (w), 2934 (w), 2842 (w), 1601 (w), 1496 (w), 1434 (w), 1419 (w), 1387 (w), 1368 (w), 1344 (w), 1254 (s), 1222 (m), 1147 (s), 1068 (w), 1052 (w), 1028 (s), 979 (w), 958 (w), 945 (w), 862 (w), 841 (w), 815 (w), 769 (m), 752 (m), 736 (w), 672 (w), 635 (s), 572 (m), 516 (m), 464 (w), 415 (w) cm^{-1}; ESI-MS (CH_3CN): m/z = 327.1546 (calcd for $[(\mathbf{L^2})(Cu) + H]^{2+}$: 327.1548), 358.1159 (calcd for $[(\mathbf{L^2})(Cu)_2]^{2+}$: 358.1157), 653.3026 (calcd for $[(\mathbf{L^2})(Cu)]^+$: 653.3024), 751.2002 (calcd for $[(\mathbf{L^2})(Cu)_2Cl]^+$: 751.2008), 803.2619 (calcd for $[(\mathbf{L^2})(Cu)(OTf) + H]^+$: 803.2622), 865.1837 (calcd for $[(\mathbf{L^2})(Cu)_2OTf]^+$: 865.1840).

[($\mathbf{L^2}$)($\mathbf{Cu_2}$(dppe))]($\mathbf{PF_6}$) (11). 1,2-Bis(diphenylphosphino)-ethane (7.3 mg, 18.4 μmol, 1 equiv.) dissolved in acetone (1 mL) was added to a solution of complex **9** (20 mg, 18.4 μmol) in acetone (2 mL). After stirring for 15 h the volume of the resulting solution was reduced under vacuum to 1 mL, followed by the addition of diethyl ether (20 mL) that caused the precipitation of a light yellow solid. This solid was isolated by filtration, washed with hexane and dried under vacuum yielding **11** (13.9 mg, 9.9 μmol, 54%). The diffusion of diethyl ether into a solution of **11** in acetonitrile provided light yellow crystals which were suitable for an X-ray diffraction analysis. IR (KBr): $\tilde{\nu}$ = 2967 (w), 2931 (w), 2868 (w), 1603 (w), 1484 (w), 1437 (w), 1416 (w), 1388 (w), 1369 (w), 1174 (w), 1132 (w), 1069 (w), 840 (s), 775 (w), 745 (w), 698 (w), 558 (m), 519 (w) cm^{-1}; ESI-MS (acetone): m/z = 557.1832 (calcd for $[(\mathbf{L^2})(Cu)_2(dppe)]^{2+}$: 557.1834), 653.3012 (calcd for $[(\mathbf{L^2})(Cu)]^+$: 653.3024), 1259.3291 (calcd for $[(\mathbf{L^2})(Cu)_2(dppe)(PF_6)]^+$: 1259.3315); elemental analysis (%) for $C_{63}H_{70}N_6OCu_2P_4F_{12}$: C 53.81, H 5.02, N 5.98; found C 54.19, H 5.37, N 5.94.

[(DBF-BrNPy$_2$)(Cu(NCCH$_3$))](OTf) (12). DBF-BrNPy$_2$ (52.3 mg, 117.7 μmol) and [Cu(NCCH$_3$)$_4$]OTf (44.4 mg, 117.7 μmol, 1 equiv.) were dissolved in acetonitrile (6 mL) and stirred for 4 h at room temperature. In the next step the volume of the resulting solution was reduced under vacuum to 1 mL, followed by the addition of diethyl ether (10 mL) that caused the precipitation of a yellow solid. This solid was isolated by filtration, washed with hexane and dried under vacuum to yield **12** (68 mg, 97.4 μmol, 83%). ^{1}H NMR (400.1 MHz, CD_3CN): δ = 8.65–8.51 (m, 2H, 2 × CH^{Py}), 8.03–7.98 (m, 1H, CH^{Ar}), 7.96–7.88 (m, 2H, 2 × CH^{Py}), 7.72–7.63 (m, 2H, 2 × CH^{Ar}), 7.63–7.57 (m, 2H, 2 × CH^{Py}), 7.48–7.41 (m, 2H, 2 × CH^{Py}), 7.34–7.27 (m, 1H, CH^{Ar}), 7.26–7.17 (m, 2H, 2 × CH^{Ar}), 4.78 (s, 4H, CH_2^{Py}), 1.96 ppm (s, 3H, NCCH_3); ^{13}C NMR (75.5 MHz, CD_3CN): δ = 157.4 (2 × C^{Py}), 153.4 (C^{Ar}), 150.2 (2 × CH^{Py}), 148.5 (C^{Ar}), 139.3 (2 × CH^{Py}), 135.5 (C^{Ar}), 131.2 (CH^{Ar}), 126.6 (C^{Ar}), 126.5 (C^{Ar}), 125.7 (CH^{Ar}), 125.2 (4 × CH^{Py}), 125.0 (CH^{Ar}), 121.5 (CH^{Ar}), 117.4 (CH^{Ar}), 116.7 (CH^{Ar}), 104.7 (C^{Ar}), 58.4 ppm (2 × CH_2^{Py}); ^{19}F NMR (282.4 MHz, CD_3CN): δ = −78.26 ppm. IR (ATR): $\tilde{\nu}$ = 1662 (m), 1602 (m), 1571 (w), 1497 (w), 1482 (w), 1430 (w), 1414 (w), 1339 (w), 1261 (s), 1223 (m), 1190 (m), 1155 (s), 1106 (w), 1053 (w), 1029 (s), 966 (w), 945 (w), 896 (w), 853 (w), 769 (m), 731 (w), 637 (s), 574 (w), 517 (w) cm^{-1}; ESI-MS (CH_3CN): m/z = 506.0477 (calcd for $[(DBF\text{-}BrNPy_2)(Cu)]^+$: 505.9924).

[(DBF-HTacn)(Cu(NCCH$_3$))](OTf) (13). A solution of DBF-HTacn (45 mg, 118.6 μmol) and [Cu(NCCH$_3$)$_4$]OTf (44.7 mg, 118.6 μmol, 1 equiv.) was stirred at room temperature for 4 h. The product was isolated following the same procedure as that described for complex **12**. After work-up **13** was obtained (48 mg, 75.8 μmol, 64%). ^{1}H NMR (400.1 MHz, CD_3CN): δ = 8.13–8.04 (m, 1H, CH^{Ar}), 7.90–7.81 (m, 1H, CH^{Ar}), 7.68–7.60 (m, 1H, CH^{Ar}), 7.60–7.50 (m, 1H, CH^{Ar}), 7.50–7.32 (m, 3H, 3 × CH^{Ar}) 3.80–3.65 (m, 2H, CH_2^{Tacn}), 3.48–3.36 (m, 2H, CH_2^{Tacn}), 3.33–3.13 (m, 4H, CH_2^{Tacn}, 2 × CH^{Tacn}), 2.99–2.88 (m, 2H, CH_2^{Tacn}), 2.86–2.65 (m, 4H, 2 × CH_2^{Tacn}), 1.96 (s, 3H, NCCH_3), 1.31 ppm (d, $^3J_{H,H}$ = 6.5 Hz, 12H, 4 × CH_3^{Tacn}); ^{13}C NMR (75.5 MHz, CD_3CN): δ = 156.1 (C^{Ar}), 149.3 (C^{Ar}), 138.2 (C^{Ar}), 128.7 (CH^{Ar}), 126.8 (C^{Ar}), 124.9 (C^{Ar}), 124.7 (CH^{Ar}), 124.4 (CH^{Ar}), 122.1 (CH^{Ar}), 119.1 (CH^{Ar}), 117.4 (CH^{Ar}), 112.4 (CH^{Ar}), 59.1 (2 × CH^{Tacn}), 54.1 (2 × CH_2^{Tacn}), 51.6 (2 × CH_2^{Tacn}), 51.1 (2 × CH_2^{Tacn}), 20.5 (2 × CH_3), 19.9 ppm (2 × CH_3^{Tacn}); ^{19}F NMR (282.4 MHz, CD_3CN): δ = −78.32 ppm. IR (ATR): $\tilde{\nu}$ = 2971 (w), 2933 (w), 2855 (w), 1592 (w), 1494 (w), 1451 (w), 1421 (w), 1388 (w), 1369 (w), 1348 (w), 1259 (s), 1222 (m), 1189 (m), 1144 (s), 1099 (w), 1029 (s), 961 (w), 936 (w), 835 (w), 789 (w), 753 (m), 718 (w), 694 (w), 636 (s), 572 (w), 517 (m) cm^{-1}; ESI-MS (CH_3CN): m/z = 442.1963 (calcd for $[(DBF\text{-}HTacn)(Cu)]^+$: 442.1914).

Oxygenation of 4–6, 9 and 10

A solution of **4**, **5**, **6**, **9** or **10** was prepared inside the glove box by dilution of **4** (7.2 mg), **5** (5.6 mg), **6** (5.1 mg), **9** (6.5 mg), or **10** (6.6 mg) in acetone (2 mL). An aliquot (0.2 mL) of the respective solution was taken and oxygenation was performed by rapid injection of the solution into an oxygen-saturated acetone solution (2.8 mL) at 183 K. The formation of the O_2 adduct was followed by UV/Vis spectroscopy. The final complex concentration was 0.25 mM for **4**, 0.18 mM for **5** and **6**, and 0.2 mM for **9** and **10**.

Oxygenation of 12 and 13

A solution of **12**, **13** or a 1 : 1 mixture of both complexes was prepared inside the glove box by dilution of **12** (3.77 mg), **13** (3.42 mg) or **12**/**13** (3.77 mg/3.42 mg) in 2 mL of acetone. An aliquot (0.2 mL) of the respective solution was taken and oxygenation was performed by rapid injection of the solution into an oxygen-saturated acetone solution (2.8 mL) at 183 K. The formation of the O_2 adduct was followed by UV/Vis spectroscopy. The final complex concentration was 0.18 mM for **12**, **13** and **12**/**13**.

Formation kinetics

The kinetics of formation of the O_2 adduct of **5** or **9** was monitored through the characteristic optical band at 396 nm or 393 nm at 193 K. The formation of the O_2 adduct was achieved

by the injection of a solution of **5** or **9** in a precooled oxygen-saturated acetone solution ([Cu] = 0.2 mM, 0.175 mM, 0.15 mM, 0.125 mM, 0.1 mM, 0.075 mM for **5** and [Cu] = 0.2 mM, 0.175 mM, 0.15 mM, 0.125 mM, 0.1 mM, 0.05 mM for **9**). The kinetic traces obtained under the pseudo-first-order conditions were fitted with the software UV-Visible ChemStation.

Kinetic studies on the oxidation of substrates involving the O adduct of 5 and 9

The oxygenation of **5** and **9** was performed as described above. After the full formation of the **O** adduct of **5** or **9** the excess O_2 was removed prior to the addition of substrates by purging with argon for 2 minutes. Afterwards ethylbenzene (100 equiv.), xanthene (20 equiv.), triphenylphosphine (20 equiv. for **5** and 50, 100, 150, 200 equiv. for **9**), 2,4-di-*tert*-butylphenol (5 equiv.), sodium-2,4-di-*tert*-butylphenol (5 equiv.), benzoylchloride (100 equiv.), and 4-methoxybenzaldehyde (20, 30, 40, 50 equiv. for **5** and 50, 100, 150, 200 equiv. for **9**) dissolved in 0.1 mL acetone were added and the decay of the formed **O** adduct of **5** or **9** was followed by UV/Vis spectroscopy at −90 °C.

Oxidation of the substrates involving the O_2 adducts of 5 and 9

Inside the glovebox compound **5** (31.3 mg) or **9** (32.7 mg) was dissolved in 10 mL acetone and an aliquot (3.33 mL) of the respective solution was taken and injected into an oxygen-saturated acetone solution (46.67 mL) at −90 °C (end concentration of **5** or **9** = 0.2 mM). As prior UV/Vis measurements had indicated the full formation of the **O** adduct of **5** within 200 s or **9** within 255 s, after addition of **5** or **9** to the oxygen-saturated acetone solution the reaction mixture was stirred for 200 s or 255 s before excess O_2 was removed by ten cycles of vacuum/Ar purging. Subsequently, the substrate (xanthene (20 equiv.), triphenylphosphine (50 equiv.), 2,4-di-*tert*-butylphenol (5 equiv.), sodium-2,4-di-*tert*-butylphenol (5 equiv.), 4-methoxybenzaldehyde (20 equiv.)) dissolved in 1.67 mL acetone was added. The reaction mixture was stirred for one hour at −90 °C and warmed to room temperature. After adding one equivalent of 1,3,5-trimethoxybenzene or diphenyl(2,4,6-trimethylbenzoyl)phosphine oxide as an internal standard, the resulting solutions were filtered through silica. After evaporation of the solvent the residues were dissolved in $CDCl_3$ and the products were analyzed by ^1H NMR and in the case of 4-methoxybenzaldehyde also by GC-MS.

Conflicts of interest

There are no conflicts to declare.

Acknowledgements

We are grateful to the Cluster of Excellence "Unifying Concepts in Catalysis" funded by the Deutsche Forschungsgemeinschaft (DFG) as well as the Humboldt-Universität zu Berlin for financial support.

References

1 (*a*) B. Hazes, K. H. Kalk, W. G. Hol, K. A. Magnus, C. Bonaventura, J. Bonaventura and Z. Dauter, *Protein Sci.*, 1993, **2**, 597–619; (*b*) K. A. Magnus, H. Ton-That and J. E. Carpenter, *Chem. Rev.*, 1994, **94**, 727–735.

2 (*a*) R. Balasubramanian and A. C. Rosenzweig, *Acc. Chem. Res.*, 2007, **40**, 573–580; (*b*) S. M. Smith, S. Rawat, J. Telser, B. M. Hoffman, T. L. Stemmler and A. C. Rosenzweig, *Biochemistry*, 2011, **50**, 10231–10240; (*c*) R. L. Lieberman and A. C. Rosenzweig, *Nature*, 2005, **434**, 177–182.

3 C. Citek, B.-L. Lin, T. E. Phelps, E. C. Wasinger and T. D. P. Stack, *J. Am. Chem. Soc.*, 2014, **136**, 14405–14408.

4 (*a*) E. I. Solomon, D. E. Heppner, E. M. Johnston, J. W. Ginsbach, J. Cirera, M. Qayyum, M. T. Kieber-Emmons, C. H. Kjaergaard, R. G. Hadt and L. Tian, *Chem. Rev.*, 2014, **114**, 3659–3853; (*b*) R. E. Stenkamp, *Chem. Rev.*, 1994, **94**, 715–726.

5 (*a*) C. Belle and J.-L. Pierre, *Eur. J. Inorg. Chem.*, 2003, 4137–4146; (*b*) N. Mitić, S. J. Smith, A. Neves, L. W. Guddat, L. R. Gahan and G. Schenk, *Chem. Rev.*, 2006, **106**, 3338–3363; (*c*) J. A. Tainer, E. D. Getzoff, J. S. Richardson and D. C. Richardson, *Nature*, 1983, **306**, 284–287.

6 (*a*) C. E. Elwell, N. L. Gagnon, B. D. Neisen, D. Dhar, A. D. Spaeth, G. M. Yee and W. B. Tolman, *Chem. Rev.*, 2017, **117**, 2059–2107; (*b*) E. A. Lewis and W. B. Tolman, *Chem. Rev.*, 2004, **104**, 1047–1076; (*c*) L. M. Mirica, X. Ottenwaelder and T. D. P. Stack, *Chem. Rev.*, 2004, **104**, 1013–1046.

7 J. N. Hamann, B. Herzigkeit, R. Jurgeleit and F. Tuczek, *Coord. Chem. Rev.*, 2017, **334**, 54–66.

8 (*a*) I. Garcia-Bosch, A. Company, J. R. Frisch, M. Torrent-Sucarrat, M. Cardellach, I. Gamba, M. Güell, L. Casella, L. Que, X. Ribas, *et al.*, *Angew. Chem., Int. Ed.*, 2010, **49**, 2406–2409, (*Angew. Chem.*, 2010, **122**, 2456–2459); (*b*) M. Mahroof-Tahir and K. D. Karlin, *J. Am. Chem. Soc.*, 1992, **114**, 7599–7601; (*c*) N. N. Murthy, M. Mahroof-Tahir and K. D. Karlin, *Inorg. Chem.*, 2001, **40**, 628–635; (*d*) M. S. Nasir, K. D. Karlin, D. McGowty and J. Zubieta, *J. Am. Chem. Soc.*, 1991, **113**, 698–700; (*e*) J. Serrano-Plana, I. Garcia-Bosch, A. Company and M. Costas, *Acc. Chem. Res.*, 2015, **48**, 2397–2406; (*f*) Y. Tachi, Y. Matsukawa, J. Teraoka and S. Itoh, *Chem. Lett.*, 2009, **38**, 202–203.

9 I. Garcia-Bosch, X. Ribas and M. Costas, *Eur. J. Inorg. Chem.*, 2012, 179–187.

10 J. Serrano-Plana, M. Costas and A. Company, *Inorg. Chem.*, 2014, **53**, 12929–12938.

11 (*a*) M. R. Halvagar, B. Neisen and W. B. Tolman, *Inorg. Chem.*, 2013, **52**, 793–799; (*b*) F. Heims, V. Mereacre, A. Ciancetta, S. Mebs, A. K. Powell, C. Greco and K. Ray, *Eur. J. Inorg. Chem.*, 2012, 4565–4569.

12 (*a*) C. E. Elwell, N. L. Gagnon, B. D. Neisen, D. Dhar, A. D. Spaeth, G. M. Yee and W. B. Tolman, *Chem. Rev.*, 2017, **117**, 2059–2107; (*b*) E. A. Lewis and W. B. Tolman, *Chem. Rev.*, 2004, **104**, 1047–1076; (*c*) L. M. Mirica, X. Ottenwaelder and T. D. P. Stack, *Chem. Rev.*, 2004, **104**, 1013–1046.

13 *Concepts and models in bioinorganic chemistry*, ed. H.-B. Kraatz and N. Metzler-Nolte, Wiley-VCH, Weinheim, 2006, pp. 363–395.

14 (*a*) W. Kaim and J. Rall, *Angew. Chem., Int. Ed. Engl.*, 1996, **35**, 43–60, (*Angew. Chem.*, 1996, **108**, 47–64); (*b*) *Handbook of Metalloproteins*, ed. A. Messerschmidt, R. Huber, T. Poulas, K. Wieghardt, M. Cygler and W. Bode, Wiley, Chichester, 2001, vol. 2, pp. 1301–1329; (*c*) M. Pascaly, I. Jolk and B. Krebs, *Chem. Unserer Zeit*, 1999, **33**, 334–341; (*d*) M. Rolff, J. Schottenheim, H. Decker and F. Tuczek, *Chem. Soc. Rev.*, 2011, **40**, 4077–4098; (*e*) E. I. Solomon, P. Chen, M. Metz, S.-K. Lee and A. E. Palmer, *Angew. Chem., Int. Ed.*, 2001, **40**, 4570–4590, (*Angew. Chem.*, 2001, **113**, 4702–4724); (*f*) E. I. Solomon, U. M. Sundaram and T. E. Machonkin, *Chem. Rev.*, 1996, **96**, 2563–2606.

15 P. L. Holland and W. B. Tolman, *Coord. Chem. Rev.*, 1999, **190–192**, 855–869.

16 T. D. P. Stack, *Dalton Trans.*, 2003, **94**, 1881–1889.

17 (*a*) H.-C. Liang, C. X. Zhang, M. J. Henson, R. D. Sommer, K. R. Hatwell, S. Kaderli, A. D. Zuberbühler, A. L. Rheingold, E. I. Solomon and K. D. Karlin, *J. Am. Chem. Soc.*, 2002, **124**, 4170–4171; (*b*) G. Y. Park, M. F. Qayyum, J. Woertink, K. O. Hodgson, B. Hedman, A. A. Narducci Sarjeant, E. I. Solomon and K. D. Karlin, *J. Am. Chem. Soc.*, 2012, **134**, 8513–8524; (*c*) J. Cahoy, P. L. Holland and W. B. Tolman, *Inorg. Chem.*, 1999, **38**, 2161–2168; (*d*) M. J. Henson, M. A. Vance, C. X. Zhang, H.-C. Liang, K. D. Karlin and E. I. Solomon, *J. Am. Chem. Soc.*, 2003, **125**, 5186–5192; (*e*) D. Maiti, J. S. Woertink, A. A. Narducci Sarjeant, E. I. Solomon and K. D. Karlin, *Inorg. Chem.*, 2008, **47**, 3787–3800.

18 (*a*) V. Mahadevan, M. J. Henson, E. I. Solomon and T. D. P. Stack, *J. Am. Chem. Soc.*, 2000, **122**, 10249–10250; (*b*) C. Citek, J. B. Gary, E. C. Wasinger and T. D. P. Stack, *J. Am. Chem. Soc.*, 2015, **137**, 6991–6994; (*c*) C. Citek, S. Herres-Pawlis and T. D. P. Stack, *Acc. Chem. Res.*, 2015, **48**, 2424–2433.

19 W. B. Tolman, *Acc. Chem. Res.*, 1997, **30**, 227–237.

20 S. Mahapatra, S. Kaderli, A. Llobet, Y.-M. Neuhold, T. Palanch, J. A. Halfen, V. G. Young, T. A. Kaden, L. Que, A. D. Zuberbühler, *et al.*, *Inorg. Chem.*, 1997, **36**, 6343–6356.

21 (*a*) J. A. Halfen, S. Mahapatra, E. C. Wilkinson, S. Kaderli, V. G. Young, L. Que, A. D. Zuberbühler and W. B. Tolman, *Science*, 1996, **271**, 1397–1400; (*b*) S. Mahapatra, J. A. Halfen, E. C. Wilkinson, G. Pan, X. Wang, V. G. Young, C. J. Cramer, L. Que and W. B. Tolman, *J. Am. Chem. Soc.*, 1996, **118**, 11555–11574.

22 (*a*) X. Ottenwaelder, D. J. Rudd, M. C. Corbett, K. O. Hodgson, B. Hedman and T. D. P. Stack, *J. Am. Chem. Soc.*, 2006, **128**, 9268–9269; (*b*) L. M. Mirica, D. J. Rudd, M. A. Vance, E. I. Solomon, K. O. Hodgson, B. Hedman and T. D. P. Stack, *J. Am. Chem. Soc.*, 2006, **128**, 2654–2665.

23 L. Q. Hatcher and K. D. Karlin, *J. Biol. Inorg. Chem.*, 2004, **9**, 669–683.

24 J. L. Que and W. B. Tolman, *Angew. Chem., Int. Ed.*, 2002, **41**, 1114–1137, (*Angew. Chem.*, 2002, **114**, 1160–1185).

25 (*a*) M. Suzuki, *Acc. Chem. Res.*, 2007, **40**, 609–617; (*b*) M. T. Kieber-Emmons, J. W. Ginsbach, P. K. Wick, H. R. Lucas, M. E. Helton, B. Lucchese, M. Suzuki, A. D. Zuberbühler, K. D. Karlin and E. I. Solomon, *Angew. Chem., Int. Ed.*, 2014, **53**, 4935–4939, (*Angew. Chem. Int. Ed. Engl.*, 2014, **126**, 5035–5039).

26 (*a*) P. Haack, A. Kärgel, C. Greco, J. Dokic, B. Braun, F. F. Pfaff, S. Mebs, K. Ray and C. Limberg, *J. Am. Chem. Soc.*, 2013, **135**, 16148–16160; (*b*) P. Haack and C. Limberg, *Angew. Chem., Int. Ed.*, 2014, **53**, 4282–4293, (*Angew. Chem.*, 2014, **126**, 4368–4380); (*c*) P. Haack, C. Limberg, K. Ray, B. Braun, U. Kuhlmann, P. Hildebrandt and C. Herwig, *Inorg. Chem.*, 2011, **50**, 2133–2142.

27 A. Company, L. Gómez, R. Mas-Ballesté, I. V. Korendovych, X. Ribas, A. Poater, T. Parella, X. Fontrodona, J. Benet-Buchholz, M. Solà, *et al.*, *Inorg. Chem.*, 2007, **46**, 4997–5012.

28 S. T. Li, B. Braun-Cula, S. Hoof, M. Dürr, I. Ivanović-Burmazović and C. Limberg, *Eur. J. Inorg. Chem.*, 2016, 4017–4027.

29 (*a*) K. E. Dalle, T. Gruene, S. Dechert, S. Demeshko and F. Meyer, *J. Am. Chem. Soc.*, 2014, **136**, 7428–7434; (*b*) S. Itoh, H. Nakao, L. M. Berreau, T. Kondo, M. Komatsu and S. Fukuzumi, *J. Am. Chem. Soc.*, 1998, **120**, 2890–2899; (*c*) N. Kindermann, E. Bill, S. Dechert, S. Demeshko, E. J. Reijerse and F. Meyer, *Angew. Chem., Int. Ed.*, 2015, **54**, 1738–1743, (*Angew. Chem.*, 2015, **127**, 1758); (*d*) T. Osako, Y. Ueno, Y. Tachi and S. Itoh, *Inorg. Chem.*, 2003, **42**, 8087–8097.

30 H. R. Lucas, L. Li, A. A. N. Sarjeant, M. A. Vance, E. I. Solomon and K. D. Karlin, *J. Am. Chem. Soc.*, 2009, **131**, 3230–3245.

31 E. B. Schwartz, C. B. Knobler and D. J. Cram, *J. Am. Chem. Soc.*, 1992, **114**, 10775–10784.

32 (*a*) T. Kobayashi, M. Kunita, S. Nishino, H. Matsushima, T. Tokii, H. Masuda, H. Einaga and Y. Nishida, *Polyhedron*, 2000, **19**, 2639–2648; (*b*) D. G. Lonnon, D. C. Craig, S. B. Colbran and P. V. Bernhardt, *Dalton Trans.*, 2004, 778–787; (*c*) M. Schatz, M. Leibold, S. P. Foxon, M. Weitzer, F. W. Heinemann, F. Hampel, O. Walter and S. Schindler, *Dalton Trans.*, 2003, **8**, 1480–1487.

33 (*a*) V. R. de Almeida, F. R. Xavier, R. E. H. M. B. Osório, L. M. Bessa, E. L. Schilling, T. G. Costa, T. Bortolotto, A. Cavalett, F. A. V. Castro, F. Vilhena, *et al.*, *Dalton Trans.*, 2013, **42**, 7059–7073; (*b*) L. M. Berreau, J. A. Halfen, V. G. Young and W. B. Tolman, *Inorg. Chem.*, 1998, **37**, 1091–1098; (*c*) J. A. Halfen, V. G. Young and W. B. Tolman, *Angew. Chem., Int. Ed. Engl.*, 1996, **35**, 1687–1690, (*Angew. Chem., Int. Ed.*, 1996, **108**, 1832–1835); (*d*) J. L. Schneider,

J. A. Halfen, J. V. G. Young and W. B. Tolman, *New J. Chem.*, 1998, **22**, 459–466.

34 (*a*) M. F. N. N. Carvalho, M. T. Duarte, T. A. Fernandes, A. M. Galvão and A. M. Botelhodo Rego, *Inorg. Chem.*, 2010, **49**, 10330–10337; (*b*) L.-X. Hu, M. Gao, T. Wen, Y. Kang and S. Chen, *Inorg. Chem.*, 2017, **56**, 6507–6511; (*c*) J. Ni, K.-J. Wei, Y. Min, Y. Chen, S. Zhan, D. Li and Y. Liu, *Dalton Trans.*, 2012, **41**, 5280–5293; (*d*) J. I. van der Vlugt, E. A. Pidko, R. C. Bauer, Y. Gloaguen, M. K. Rong and M. Lutz, *Chem. – Eur. J.*, 2011, **17**, 3850–3854; (*e*) A. Bheemaraja, J. W. Beattie, Y. Danylyuk, J. Rochford and S. Groysman, *Eur. J. Inorg. Chem.*, 2014, 5865–5873.

35 (*a*) T. Tano, H. Sugimoto, N. Fujieda and S. Itoh, *Eur. J. Inorg. Chem.*, 2012, 4099–4103; (*b*) Y. Meesala, H.-L. Wu, B. Koteswararao, T.-S. Kuo and W.-Z. Lee, *Organometallics*, 2014, **33**, 4385–4393.

36 (*a*) B. M. T. Lam, J. A. Halfen, V. G. Young, J. R. Hagadorn, P. L. Holland, A. Lledós, L. Cucurull-Sánchez, J. J. Novoa, S. Alvarez and W. B. Tolman, *Inorg. Chem.*, 2000, **39**, 4059–4072; (*b*) L. Yang, J. Tehranchi and W. B. Tolman, *Inorg. Chem.*, 2011, **50**, 2606–2612.

37 (*a*) S. H. Strauss, *Chem. Rev.*, 1993, **93**, 927; (*b*) R. Díaz-Torres and S. Alvarez, *Dalton Trans.*, 2011, **40**, 10742–10750.

38 (*a*) V. Mahadevan, Z. Hou, A. P. Cole, D. E. Root, T. K. Lal, E. I. Solomon and T. D. P. Stack, *J. Am. Chem. Soc.*, 1997, **119**, 11996–11997; (*b*) S. Mahapatra, V. G. Young, S. Kaderli, A. D. Zuberbühler and W. B. Tolman, *Angew. Chem., Int. Ed. Engl.*, 1997, **36**, 130–133, (*Angew. Chem.*, 1997, **109**, 125–127); (*c*) H. Hayashi, S. Fujinami, S. Nagatomo, S. Ogo, M. Suzuki, A. Uehara, Y. Watanabe and T. Kitagawa, *J. Am. Chem. Soc.*, 2000, **122**, 2124–2125.

39 *Comprehensive handbook of chemical bond energies*, ed. Y.-R. Luo, CRC Press/Taylor & Francis Group, Boca Raton, 2007, pp. 255–368.

40 J. A. Halfen, W. B. Tolman and K. Weighardt, *Inorg. Synth.*, 1998, **32**, 75–81.

41 G. J. Kubas, B. Monzyk and A. L. Crumbliss, *Inorg. Synth.*, 1979, **19**, 90–92.